ELSEVIER

Contents lists available at ScienceDirect

# Journal of Hydrology

journal homepage: www.elsevier.com/locate/jhydrol



### Research papers

## Groundwater dominates terrestrial hydrological processes in the Amazon at the basin and subbasin scales

Omid Bagheri<sup>a</sup>, Yadu Pokhrel<sup>a,\*</sup>, Nathan Moore<sup>b</sup>, Mantha S. Phanikumar<sup>a</sup>

- <sup>a</sup> Department of Civil and Environmental Engineering, Michigan State University, East Lansing, MI, USA
- <sup>b</sup> Department of Geography, Environment and Spatial Science, Michigan State University, East Lansing, MI, USA

#### ARTICLE INFO

This manuscript was handled by Marco Borga, Editor-in-Chief

Keywords: Amazon basin Dominant hydrological processes Groundwater Process-based modeling Forest management

#### ABSTRACT

The hydrology of the Amazon River basin (ARB) has been extensively studied; however, critical scientific gaps remain regarding key processes that govern hydrologic dynamics and the resilience of the rainforest. This inhibits the understanding of hydrological considerations needed for sustainable forest management under climate change and growing human stressors. Here, using high resolution (~2km), long-term simulations from a processbased hydrological model (LEAF-Hydro-Flood), we investigate the dominant hydrological processes across the ARB, their key roles in shaping basin functions, and the decadal evolution therein. Results indicate that shallow groundwater (<5m deep) strongly modulates the seasonality of the surface fluxes across the ARB and at least 34% of the Amazonian Forest is supported by groundwater during the dry season. A two-month lag between the seasonal peak of evapotranspiration (ET) and river discharge is a key mechanism that potentially prevents the rainforest from tipping into savanna. The dry season in the ARB is getting drier and the wet season is getting wetter, pointing to an accelerating hydrologic cycle. The ARB is dominantly energy limited, however, our results imply that in the absence of groundwater support, and with less than ~125 mm/month of precipitation, the basin could have become water-limited over some regions. The long-term basin-averaged ET-dominated by transpiration—changed with a split pattern of  $\pm 9\%$  in the past three decades. Similarly, water table depth ( $\pm 19\%$ ) and runoff (±29%) changed with heterogenous patterns across the ARB. Further, the contribution of canopy interception loss and ground evaporation changed heterogeneously across the ARB in response to deforestation. River discharge did not change substantially due to the crucial buffering role of groundwater, but terrestrial water storage (TWS) decreased (increased) in the 2000s (2010s) compared to that in the 1990s. Although groundwater is the dominant contributor to total TWS, the dynamics of TWS over the major river channels are controlled by flood water, given relatively shallow groundwater. This study provides crucial insights on the dominant hydrological processes in the ARB to inform forest management practices.

#### 1. Introduction

The Amazon River basin (ARB) is home to the most extensive tropical forest biome on the planet (e.g., 40% of the global tropical forest area) and is also one of the tipping elements of the Earth system (Aragão et al., 2014; Laurance et al., 2001; Lenton et al., 2008; Schellnhuber, 2009; Weng et al., 2018). The basin is an important component of global biodiversity as well as global water, energy, and carbon cycles, and plays a key role in the global climate system through precipitation recycling and atmospheric moisture transport (Arvor et al., 2017; Fan and Miguez-Macho, 2010; Fassoni-Andrade et al., 2021; Laurance et al., 2002; Malhi et al., 2008; Soares-Filho et al., 2006; Werth and Avissar, 2005). The

basin functioning (e.g., carbon storage, maintenance of biodiversity, and climate regulation) in the ARB has been altered substantially over the past few decades due to climate variability and human disturbances with deforestation as the dominant form; the deforestation is primarily a result of cattle ranching and replacement of forests with pasture at the agriculture frontier ("arc of deforestation") in the southern subbasins (Bagley et al., 2014; Costa et al., 2007; Costa and Pires, 2010; Davidson et al., 2012; Guan et al., 2015; Fearnside, 2000; Moore et al., 2007; Morton et al., 2006). In addition, rapid population growth, timber extraction, mining, forest fires, and road network expansion are among other sources of land use and land cover (LULC) change in the ARB (Foley et al., 2005; Soares-Filho et al., 2006).

E-mail address: ypokhrel@msu.edu (Y. Pokhrel).

<sup>\*</sup> Corresponding author.

The hydrological cycle in the ARB is strongly modulated by evapotranspiration (ET) and frequent (up to 7 recyclings per water molecule) (Salati et al., 1979; Staal et al., 2018; Weng et al., 2018) and substantial (25-50% of total Amazonian rainfall) moisture recycling (Aragão, 2012; Eltahir and Bras, 1994; Spracklen et al., 2012; Staal et al., 2018; Van Der Ent et al., 2010; Zemp et al., 2017). Therefore, the basin's hydrologic system is highly susceptible to widespread deforestation and forest degradation because it can substantially reduce moisture availability for recycling by increasing surface runoff (Lovejoy and Nobre, 2019; Malhi et al., 2008; Schellnhuber, 2009; Zemp et al., 2017). In addition, the possibility of having positive feedback due to tree loss might exacerbate deforestation impacts (Zemp et al., 2017); tree loss reduces both ET and rainfall, lengthening dry season, reducing humidity, and potentially increasing forest fire (Zemp et al., 2017). Over most of the deforested areas in the ARB, land use is beyond moderate intensity and the hydrologic system has evolved under climate variability and anthropogenic disturbances, especially land use change (Chagas et al., 2022). For example, wet (dry) season is becoming wetter (drier) during the past decades in around one-third of the ARB (mainly in southern and eastern regions of the basin) (Leite-Filho et al., 2019) and the seasonal storage deficit has increased over time (Chaudhari et al., 2019). In addition, vapor pressure deficit (VPD) is increasing over South America (Barkhordarian et al., 2019) and mortality rate of wet-climate tree species where dry season is becoming longer is increasing (Esquivel-Muelbert et al., 2019). Moreover, due to the increase in the frequency of extreme droughts, higher temperatures and increased forest degradation, the rainforest is becoming more vulnerable to fires (Aragão et al., 2018). Therefore, over many of the deforested regions, especially in southern and eastern ARB, the hydrological system is likely being transformed with some changes being potentially irreversible (Lovejoy and Nobre,

Several studies have predicted that with the current rate of deforestation and biodiversity loss, the ARB may have two tipping points, which could lead to savannization of the bistable regions of the tropical forest through loss of moisture recycling as a result of crossing the 40% deforestation threshold (change in internal state of the system due to anthropogenic impacts) or a 4°C increase in temperature (global/ regional climatic drivers) (Cox et al., 2004; Nobre et al., 2016; Nobre and Borma, 2009; Sampaio et al., 2007; Schellnhuber, 2009; Soares-Filho et al., 2006; Staver et al., 2011; van Nes et al., 2016; Walker, 2020; Zak and Nippert, 2012). However, based on the Assessment Report 5 of the Intergovernmental Panel on Climate Change (IPCC) and by going beyond a single-factor in explaining the forest degradation and considering the combined roles of global warming, deforestations and wildfires, the threshold for deforestation has been suggested to be as low as 20-25% instead of 40%, which could push the ARB toward an opencanopy degraded state, a very likely near future scenario (Lovejoy and Nobre, 2019; Nobre et al., 2016; Walker, 2020). Other studies have shown that temperatures in the region rose by 1-1.5°C over past six decades (Nobre et al., 2016), ~18% of the forest area is deforested (Mapbiomas\_Amazonia, 2022), forest degradation reached 17% (Bullock et al., 2020; Matricardi et al., 2020), forest fires significantly increased (Aragão et al., 2018), dry season lengths (number of consecutive days with less than 50 mm rainfall) are three to four weeks longer in comparison to six decades ago (Fu et al., 2013), and dry season water storage deficit is on a divergent trend (Chaudhari et al., 2019). Some studies suggest that the increasing frequency of unprecedented droughts such as those of 2005, 2010, 2015-16 and 2020 could be signaling that the tipping point is at hand (Bagley et al., 2014; Lovejoy and Nobre, 2019; Walker, 2020). Therefore, there is a need to reduce deforestation in the ARB, rebuild the lost forest in its southern and eastern regions and to provide science-based guidelines to assist forest management policies (Lovejoy and Nobre, 2019; Walker, 2020).

Globally, passive and active approaches have been used to alleviate environmental stressors and to restore the forest through a secondary succession (Morrison and Lindell, 2011; Poorter et al., 2021). To

measure the success of forest restoration, typical characteristics such as forest structure and diversity and ecosystem functioning are compared between the old-growth forest and the secondary forest where hydrological functioning is often neglected (Poorter et al., 2021). While tree restoration has been recognized as an effective way to store carbon and mitigate the impacts of climate change, not many studies have considered the hydrological effects of tree restoration (Hoek van Dijke et al., 2022). A recent study on the impacts of large-scale tree restoration showed that restoration can significantly alter terrestrial water cycle at different spatial scales and the impacts are non-linear and complex (Hoek van Dijke et al., 2022). Traditional management policies in the ARB were commonly developed focusing on maximizing economic benefits and neglecting hydrological roles of the forest (Nobre et al., 2016). Such omission of the hydrological roles arises partly from the lack of a comprehensive understanding of the short- and long-term impacts of management practices over varying temporal and spatial scales. As such, it is imperative that we better understand the dominant hydrological processes across the ARB that govern forest resilience and are crucial for improved management practices. In addition, since forest management can have long-term implications on the future of the ARB, it is important that such studies investigate the decadal evolution of the dominant processes under climate variability and human disturbances. Lastly, identifying warning signals can help better monitor the impacts of management policies on the terrestrial hydrological cycle.

However, observational data-even those based on remote sensing—for such long-time scales and all relevant hydrological variables are lacking, especially for the entire ARB, or are available at short temporal scales, which make hydrological modeling the only viable option to study the terrestrial hydrology of the ARB. Early hydrological modeling studies in the ARB were conducted to uncover the underlying processes involved in moisture recycling and to study the impact of LULC change on the water cycle (Costa and Foley, 1999; Eltahir and Bras, 1994; Nobre et al., 1991; Shukla et al., 1990; Zeng, 1999; Zeng et al., 1996). These studies have emphasized the importance of land--atmosphere feedback in hydrological modeling to reduce the uncertainty in the results as some earlier studies found contradictory outcomes associated with neglecting the feedback (Eltahir and Bras, 1994). The limitations in required data and computational resources to run distributed hydrological land surface models in the past lead to significant growth of lumped hydrological models and data-based studies in the ARB. Lumped models are valuable tools to understand the big picture of hydrology in the ARB and to address wide range of research questions, however, they do not fully account for the heterogeneity in biomes and are simplistic in parameterizing various storages and fluxes, making them inappropriate for studies on process characterization (Heerspink et al., 2020; Maeda et al., 2017).

Advances in process-based hydrological modeling and remote sensing methods have provided new opportunities to simulate basin hydrology and study the dominant terrestrial hydrological processes (Clark et al., 2015; De Paiva et al., 2013; Frappart et al., 2019; Getirana et al., 2012; Pfeffer et al., 2014). Such models have been used to simulate groundwater dynamics across the ARB, leading to fundamental advances in the understanding of the role of groundwater and providing opportunities to disentangle research questions that were not possible to address before (Chaudhari et al., 2021; Miguez-Macho and Fan, 2012a, b; Pokhrel et al., 2014, Pokhrel et al., 2013). For example, Miguez-Macho and Fan (2012a) investigated the role of groundwater on the surface water dynamics of the ARB and the buffering role of groundwater during the dry season based on the results of LEAF-Hydro-Flood (LHF) simulations. They found that the dynamics of WTD dominates streamflow in the headwater catchments and the two-way exchanges of surface and subsurface water over the large floodplains. In addition, shallow WTD supports large areas of waterlogged wetlands that are rarely flooded. In a following study, Miguez-Macho and Fan (2012b) investigated the role of groundwater in mitigating water stress on related processes to soil moisture and ET. Further, Pokhrel et al. (2013), studied the influence of groundwater on terrestrial water storage (TWS) using LHF model, finding that subsurface storage dominates the dynamics of TWS over a major part of the ARB; however, they reported that where WTD is shallow, the dynamics of TWS is governed by floodwater. In another study and based on the results of the LHF model, Chaudhari et al. (2019) investigated the dominant mechanisms modulating the dynamics of TWS and droughts over the ARB. They suggested that the ARB is getting wetter overall, but the southern and southeastern subbasins are getting drier with the dry season water storage deficit on a divergent trend. A recent study suggests that the double stress of waterlogging and drought is the primary driver of forest-savanna coexistence with alternating drought and waterlogging at the seasonal scale favoring savanna over forests (Mattos et al., 2023). Despite the findings in recent studies, to the best of our knowledge, there are no comprehensive studies that investigated the key processes governing the hydrologic dynamics at the basin and subbasin scales across the ARB, the linkages therein, and their historical evolution.

The present study addresses the aforementioned research and knowledge gaps by answering the following science questions. (1) How did the fundamental hydrological processes in the ARB evolve over the past three decades? (2) What key factors govern the seasonality of the ARB at the basin and subbasin scales? (3) To what extent can hydrological variables in the ARB serve as viable early or late warning signals of alterations in the terrestrial water cycle during secondary succession? (4) What are the implications for forest management that can be derived from the findings of studies such as ours? We hypothesize that the shallow water table depth (WTD<5m) was a key attribute that supported the ARB's hydrologic regime during the past three decades against climate variability and anthropogenic disturbances. As such, shallow groundwater fraction area could be taken as a proxy to monitor the impacts of human activities on the basin's hydrology and ecosystem functioning. Our second hypothesis is that the changes in the spatial distribution of ET serve as a direct measure of the hydrological impact of large-scale LULC changes in the basin. In addressing these questions and hypotheses, we first identify the dominant hydrological mechanisms by using the results from a basin-scale, fully process-based hydrological model. Then, we investigate how the key hydrological processes have evolved over the last three decades. Finally, we examine the role of the governing hydrological processes for sustainable forest management in the ARB.

#### 2. Methods

### 2.1. Model description

The model used in this study is LHF (Miguez-Macho and Fan, 2012a, b; Pielke et al., 1992; Pokhrel et al., 2014, 2013; Walko et al., 2000). As described in detail in Miguez-Macho and Fan (2012a), LHF is a fully process-based hydrology model capable of resolving coupled surface and subsurface hydrological processes at the continental-scale. The was developed at two stages building on Land-Ecosystem-Atmosphere Feedback (LEAF), the land-surface component of Regional Atmosphere Modeling System (RAMS) (Walko et al., 2000). The physics in the original LEAF model is described in detail in Walko et al. (2000). Turbulent and radiative exchange of the atmosphere with multilayer soil and snow water and thermal energy, surface storage, vegetation canopy, canopy air are inherited features of LEAF in LHF (Miguez-Macho and Fan, 2012a,b). These include the parameterizations for simulating ET, which are similar to those used in state-of-the-art land surface models (e.g., Lawrence et al., 2019); details are available in Walko et al. (2000). However, LEAF parameterizations including representation of sub-grid hydrologic heterogeneity, lateral soil water movement based on TOPMODEL (Beven and Kirkby, 1979) and groundwater flow processes have been replaced with new schemes or largely improved. The new developments and enhancements have been particularly tested over the ARB as described in the following.

At the first stage of LHF development over North America (Miguez-Macho et al., 2007), LEAF-Hydro was adapted from LEAF by adding a prognostic groundwater module to allow (1) the rise and fall of water table or shrinkage and growth of the vadose zone, (2) the recharged water table to reach a new equilibrium following a rain event by discharging into rivers within a grid cell and convergence and divergence of lateral flow among adjacent cells, (3) two-way exchange between surface water and groundwater to represent both gaining and losing streams, (4) river routing to the ocean using the kinematic wave method and (5) sea level to influence coastal drainage by assigning the sea level as the groundwater head boundary condition. During the second stage over the ARB (Miguez-Macho and Fan, 2012a,b), LHF was developed through further enhancement of LEAF-Hydro by incorporating a river-floodplain routing scheme to estimate streamflow more realistically by solving the full momentum equations of open channel flow, also considering back water effect and the inertia of deep flow, which are both significant in the ARB (Bates et al., 2010; Miguez-Macho and Fan, 2012a,b; Yamazaki et al., 2011). The incorporation of flood dynamics also enabled an explicit simulation of floodwater-groundwater interactions, a dominant process in the ARB. The initial LHF studies over the ARB provided an extensive evaluation of many hydrologic variables across the basin (Miguez-Macho and Fan, 2012a,b). The model was subsequently used in numerous studies that presented further evaluations using observational and satellite-based data on various hydrologic fluxes and stores, and by using different atmospheric forcing datasets demonstrating robust model performance over the ARB (Brown et al., 2022; Chaudhari et al., 2021, 2019; Chaudhari and Pokhrel, 2022; Miguez-Macho and Fan, 2012a,b; Pokhrel et al., 2014, 2013).

#### 2.2. Atmospheric forcing

LHF model in this study is forced with ERA5 reanalysis (Hersbach et al., 2020) available from 1950 to present at the spatial resolution of 0.25 degree and hourly time steps. The availability period and the spatial resolution were the main reasons for using EAR5 data. In previous studies, LHF results forced by WATCH Forcing Data methodology applied to ERA-Interim (WFDEI) reanalysis were successfully validated over ARB, however, the dataset is not available after 2019 (Chaudhari et al., 2019). Staal et al. (2020) used ERA5 over the ARB to conduct hydrological and atmospheric moisture tracking simulations and their results showed that ERA5 performs better than ERA-Interim in estimating wind fields and rainfall, especially in tropics (Staal et al., 2020). A total of eight variables from ERA5 dataset are used: precipitation, surface pressure, surface solar (i.e., shortwave) radiation downwards, surface thermal (i.e., longwave) radiation downwards, air temperature, dewpoint temperature, u- and v-components of wind speed. Specific humidity is calculated from dewpoint temperature and surface pressure. The 3-hourly data at the coarser resolution noted above are spatially interpolated within LHF to the model grid resolution (~2km) using a bilinear interpolation (Chaudhari et al., 2021; Pokhrel et al., 2013, 2014; Miguez-Macho and Fan, 2012a).

### 2.3. Land Use/Land cover and LEAF area index

The annual LULC maps are derived from the European Space Agency (ESA) Climate Change Initiative's Land Cover project; the original data are reclassified and aggregated to match the land use categories used in LHF, following our previous study (Chaudhari et al., 2019). Specifically, the 22 classes from the ESA land cover maps are reclassified into the 30 classes of LHF (Table S3). The datasets comprise an annual time series land cover maps with 300-meter spatial resolution for the 1992 to 2020 period. The baseline maps in the ESA dataset are generated using the Medium-spectral Resolution Imaging Spectrometer (MERIS) instrument based on the UN Land Cover Classification System (LCCS) and the maps were further modified based on the detected changes in LULC by AVHRR (1992–1999), SPOT-Vegetation (1999–2012), and PROBAV

(2013–2020) instruments. The LHF model updates LULC on an annual basis to account for year-to-year LULC changes; in the ARB, these annual changes are largely caused by human activities. The lookup table for leaf area index (LAI) is derived by overlaying the ESA land use map over the LAI maps from Moderate Resolution Imaging Spectroradiometer (MODIS) for the period of 2000 to 2020 and using a pixel-by-pixel analysis and the monthly values (Table S4) are calculated from the long-term 4-day mode of LAI for each LHF land cover class.

#### 2.4. Simulation setup

The LHF model is set up for the entire ARB ( $\sim$ 7.1 million km²) including the Tocantins River basin (Fig. 1). Simulations are conducted for the 1979–2020 period at a spatial resolution of 1 arcmin ( $\sim$ 2km) with a time step of 4 minute as in previous studies (Chaudhari et al., 2019; Pokhrel et al., 2013, 2014; Miguez-Macho and Fan, 2012a), and the output is saved at daily time steps. To capture the hillslope processes at up to the first-order stream valleys, very fine spatial scale for the simulations is desired, however, due to the computational costs and the coarse resolution of input data (such as soil characteristics) the spatial

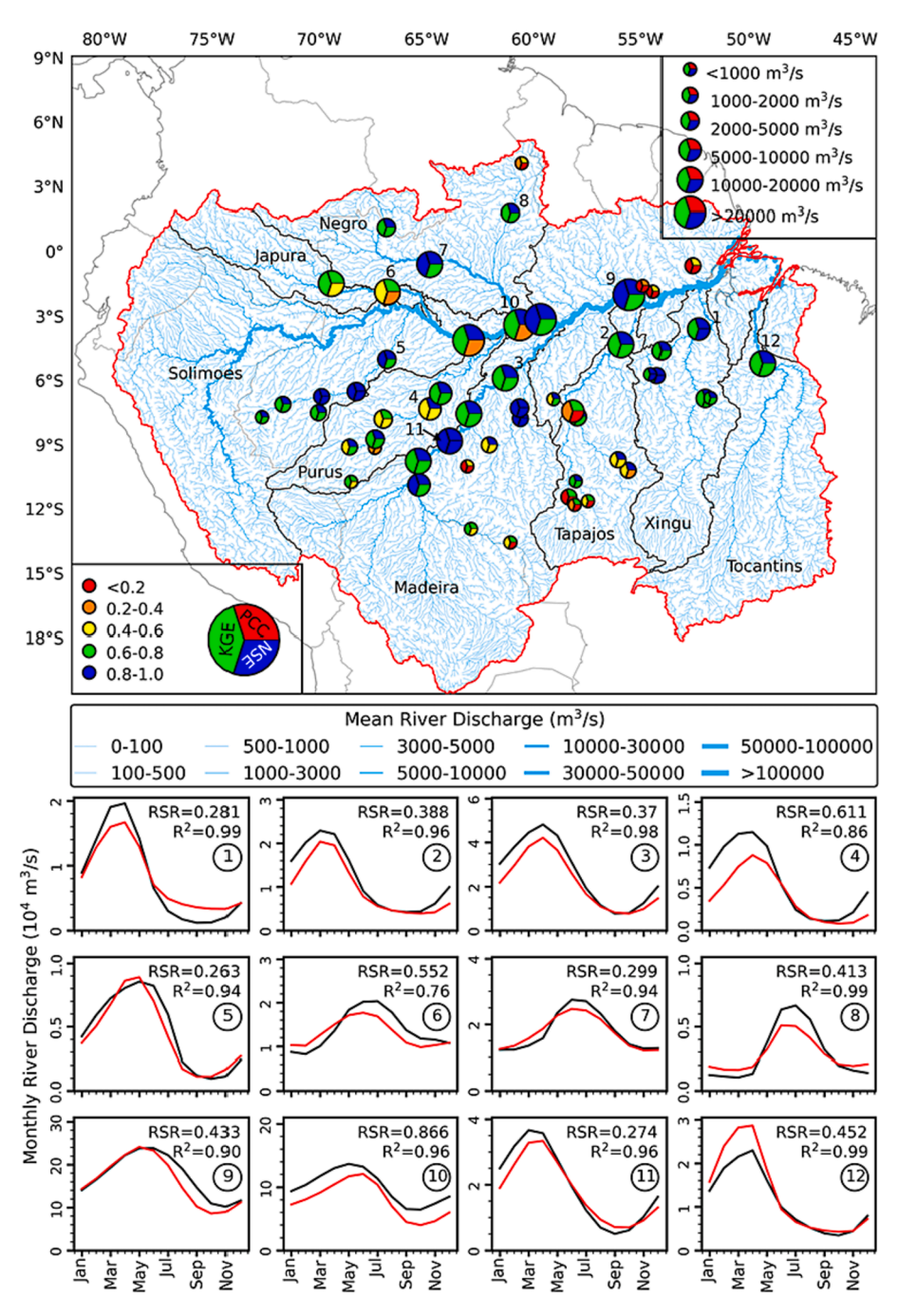


Fig. 1. River discharge validation based on monthly average values derived from daily river discharges at 55 gauge stations across the ARB. The size of the circles in the top panel indicates flow magnitude with each of the three portions of the circles showing a model performance metric: PCC (red), KGE (green), and NSE (blue). The background image shows simulated river discharge indicated by line thickness (~2km grids). The grid panels at the bottom depict the long-term seasonal cycle of monthly river discharge for 12 major gauge stations indicated on the top panel. (For interpretation of the references to colour in this figure legend, the reader is referred to the web version of this article.)

resolution of 1 arcmin is chosen as a tradeoff, as in previous studies. Reservoirs are not considered in the simulation, however, based on previous studies the impact of the reservoirs in the ARB are not substantial in the downstream reaches (Chaudhari and Pokhrel, 2022). As the focus of this study is to investigate the terrestrial hydrological processes at basin and subbasin scales, the impacts of reservoirs would not alter the findings. Starting with the equilibrium water table (Fan et al., 2013) for 1979, the model is spun up for  $\sim\!200$  times for the year 1979 to stabilize WTD and the results for the 1992–2020 period (28 years) are analyzed. As the primary goal of this study is to examine the dominant processes in the ARB on a decadal scale and since the land cover and LAI datasets are available after 1992, simulations for 1979 to 1992 are discarded as additional spin-up. Moreover, as the model simulates land surface, hydrologic, and groundwater processes on a full physical basis, no calibration was performed (Chaudhari et al., 2019).

### 2.5. Trend analysis

The Mann-Kendall (MK) test (Kendall, 1948; Mann, 1945) which serves as a prevalent method for detecting alterations in time-series data (Li et al., 2014) is used to detect the long-term trend. In this study, the detected trend is deemed statistically significant when the p value is less than 0.05 (i.e., 95% confidence level). Moreover, we employ the Theil-Sen slope estimator (Sen, 1968; Theil, 1950) to calculate the slope of change which computes the median slopes of lines fitted through pairs of data points in the dataset. Importantly, it exhibits greater robustness against outliers compared to simple linear regression methods (Lavagnini et al., 2011). The outcomes of the MK test are interpreted utilizing the z-score metric, wherein the sign of the z-score denotes the direction and magnitude of the trend. To comprehensively address the heterogeneity observed in the changes across key hydrological variables in our study, we calculate the mean slope separately for areas exhibiting negative and positive slopes. Additionally, we compute the basinaveraged slope to provide a more intricate understanding of the transformations occurring over the past three decades within the ARB.

#### 3. Results and discussion

#### 3.1. Validation

The simulated streamflow from LHF is compared with observations obtained from the Agência Nacional de Águas (ANA) in Brazil (https://www.gov.br/ana/pt-br, last accessed: 10 September 2022). In this regard, 55 stream gauging stations from a wide range of river discharge magnitudes with at least 30 years of record are considered across the ARB. Fig. 1 presents the results of three performance metrics, namely the Pearson correlation coefficient (PCC), modified Kling-Gupta efficiency (KGE) and Nash-Sutcliffe efficiency (NSE) (Sigueira et al., 2018). High values for PCC, KGE and NSE metrics can be observed for most stations, indicating overall good performance for various topographic locations and river discharge values. However, there are some stations with relatively lower PCC, KGE and NSE, which are situated mostly in streams with low annual mean flow and steep slopes, including the headwaters across the Andes in Japura and Negro subbasins and along the streams in the northeastern regions of the ARB. The lower accuracy at those stations is likely related to high topographic gradient, where precipitation drains quickly, causing rather erratic patterns of seasonal streamflow, which adds challenges to resolving hillslope processes for low order streams at 2km resolution. In addition to the above statistical measures, the long-term seasonality of streamflow for 12 major gauge stations is compared (Fig. 1). R-squared and RSR (a standardized version of the root mean square error (RMSE) that takes the standard deviation of the observed data at different stations into account (Legates and McCabe, 1999)) indicate good model performance in predicting the streamflow seasonality.

As shown in previous studies (Chaudhari et al., 2019; Felfelani et al.,

2017; Pokhrel et al., 2013) and corroborated in this study (Section 3.2), groundwater is the major component of TWS in the ARB because over most parts of the basin the water table is relatively shallow. Therefore, given the lack of systematic water level observations in the ARB, TWS validation can be used as a proxy for groundwater validation. Comparison of TWS anomalies between LHF simulations and GRACE data (Fig. 2) shows a high level of agreement for the basin-averaged anomalies and for most of the eight subbasin-averaged anomalies. However, at some of the subbasins there are some differences which are likely caused by the biases in forcing data, imperfect model parameterizations, and potential biases in GRACE data for small subbasins (Chaudhari et al., 2019, 2018; Felfelani et al., 2017; Longuevergne et al., 2010) such as Tocantins. However, in all subbasins the simulated TWS follows the patterns of precipitation anomalies (grey bars in Fig. 2), further suggesting that some of the discrepancies could be attributed to precipitation biases. The model performs better in the first half of the simulation period in comparison to the second half, especially in the western subbasins including Solimoes and Japura, which could be partially attributed to the decreasing trend in precipitation in the first half of the simulation period (Figure S2).

The model simulates the seasonality of TWS very well in comparison to GRACE (low RSR and high  $R^2$ ; Fig. 2), which adds more confidence to the results of this study as the seasonality is a key focus area in this study (Fig. 2). The seasonal cycle of TWS components shows the dominant role of groundwater storage in governing TWS changes in the majority of the subbasins, especially in the subbasins with relatively deep groundwater (WTD>2m) such as Tocantins, Tapajos, and Xingu. However, in the subbasins where the groundwater is relatively shallow, flood water storage plays an equally prominent role in modulating TWS anomalies (e.g., Solimoes, Purus, and Negro). We note that because soil moisture storage in LHF is defined as the moisture above WTD, the seasonal cycles of groundwater and soil moisture storage have an inverse relationship.

Decadal mean of the spatial distribution of ET is validated against MODIS MOD16A3GF Version 6.1 (Running et al., 2021) product, a yearend and gap-filled yearly composite dataset produced at 500m resolution for the period of 2000-present (Fig. 3A). The comparison of longterm annual mean of ET between the LHF simulation results (Fig. 3B) and MODIS data shows a good agreement (Fig. 3D). However, there are notable differences over certain areas which include flood-dominated regions, grasslands, and shrublands (Figure S2). These differences could be attributed to the differences in the way ET is estimated. The annual MODIS ET was derived based on the Penman-Monteith equation (Monteith, 1965), which includes inputs of daily meteorological reanalysis data along with MODIS remotely sensed data products such as dynamic vegetation properties, albedo, and land cover (Running et al., 2021). ET in LHF is, however, calculated based on energy balance approach (Miguez-Macho et al., 2007; Walko et al., 2000). Another source of discrepancy is the different in spatial resolution between the two products; model results could have higher uncertainties in regions within waterbodies including, river channels, lakes, and wetlands, where MODIS product might have accurately captured the ET dynamics. In addition to MODIS ET, the long-term annual mean of ET is compared with The Global Land Evaporation Amsterdam Model (GLEAM; Fig. S3C) V3.8a (Martens et al., 2017; Miralles et al., 2011) product, a set of algorithms to estimate daily components of land evaporation at 0.25 degree grid cell from satellite and reanalysis data for the period of 1980present based on the Priestly and Tylor equation (Priestley and Taylor, 1972) and Gash's analytical model (Gash, 1979). The comparison of long-term annual mean of ET between the LHF simulation results and GLEAM data shows a better agreement than MODIS over most of the ARB (Fig. S3E). However, along the northern boundary of the ARB, the comparison shows more discrepancy in comparison to MODIS. A further investigation by comparing MODIS and GLEAM datasets shows that there are notable discrepancies even between the two datasets (Fig. S3F), making it difficult to draw a clear conclusion on model performance. In general, given that MODIS and GLEAM ET are also

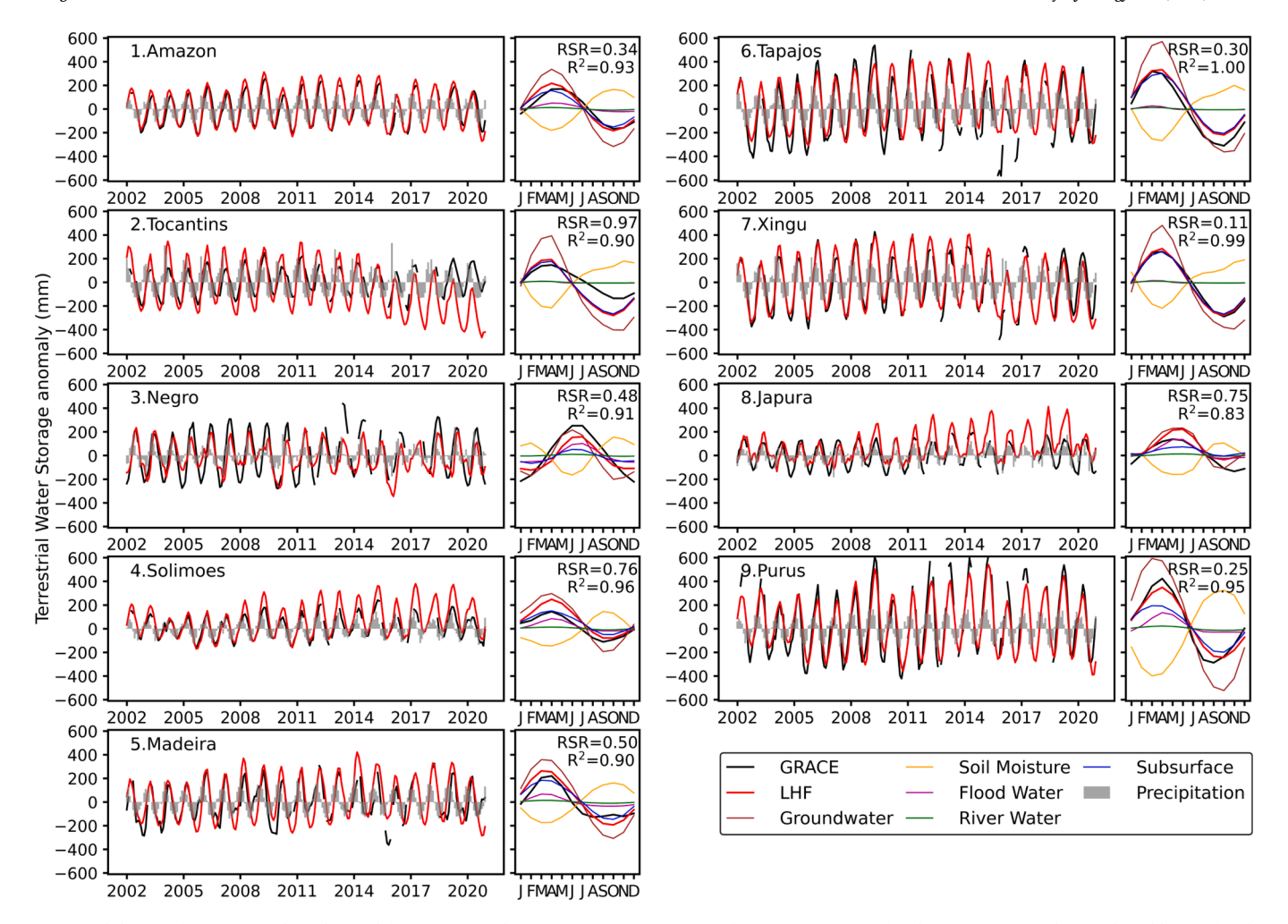


Fig. 2. Validation of TWS anomalies obtained from LHF simulations against GRACE anomalies (CSR Mascons) for the entire ARB and its eight subbasins for the period of 2002–2020. Basin and subbasin-averaged precipitation anomalies are obtained from ERA5 dataset (grey bars). Seasonal cycles of GRACE and simulated TWS and its components are shown in the right panel of each time series. GRACE results are shown as the mean of mascon solutions and simulated TWS anomalies are calculated with respect to the anomaly window of 2004–2009 for consistency with GRACE.

estimates—not true observations—that is known to include uncertainties (Xu et al., 2019), these comparisons demonstrate that the simulated ET is not out of bounds (Fig. 3) and add further confidence to the results of this study.

Overall, the evaluation of river discharge, TWS, and ET with multiple independent products, in addition to a substantial validation presented in multiple previous studies (Chaudhari et al., 2019; Pokhrel et al., 2013, 2014; Miguez-Macho and Fan, 2012a), presents sufficient basis on the usefulness of the model to study the dominant hydrological processes and their spatial and temporal variability across the ARB. Further, given that the model is fully physically based, not calibrated with observations, and applied over a large domain of the ARB, we consider the model performance to be satisfactory for our application.

## 3.2. Dynamics of key hydrological processes

In this section we address the first research question by presenting an in-depth analysis of the dynamics of key hydrological processes within the ARB over the last three decades with a focus on various water and energy balance components and associating the changes in these components with major hydrologic drivers. The dynamics of the hydrological functioning of the basin, driven by climatic and anthropogenic factors, have substantial implications for forest and ecosystem management of the ARB. Exploring the shifts in these processes provides insights into the basin's sensitivity to climatic change, the impacts of

human activities, and overall forest resilience. The subsequent subsections unravel the details of each hydrological component, shedding light on the interplay among them and implications for forest management.

### 3.2.1. Dynamics of groundwater mechanisms

The hydrological dynamics within the ARB have undergone substantial changes over the past three decades (Fig. 4). The variations in WTD across the ARB exhibit a remarkable spatial heterogeneity from east to west, serving diverse functions and roles (Fig. 4F). The WTD varies, with shallow water tables (WTD<5m) found predominantly in the central and northwestern regions, and deeper water tables (5m<WTD<20m) in the southeastern parts. This spatial pattern, consistent with earlier studies (Miguez-Macho and Fan, 2012a; Fan et al., 2013), underscores the prevalence of deep groundwater in the headwater catchments of the basin, notably influencing headwater streamflow (Frappart et al., 2019; Miguez-Macho and Fan, 2012a). In the low-lying floodplains, groundwater-surface water interactions regulate seasonal hydrologic dynamics, converting groundwater storage into a sink during the wet season and a source during the dry season—a key mechanism that sustains baseflow (Miguez-Macho and Fan, 2012a).

The basin-averaged WTD over the ARB changed with a heterogenous pattern ( $\pm 19\%$ ) during the past three decades. A notable decline in WTD over the past three decades with an average slope of 69 mm/year over these regions is apparent (Fig. 4L), with the trend being statistically

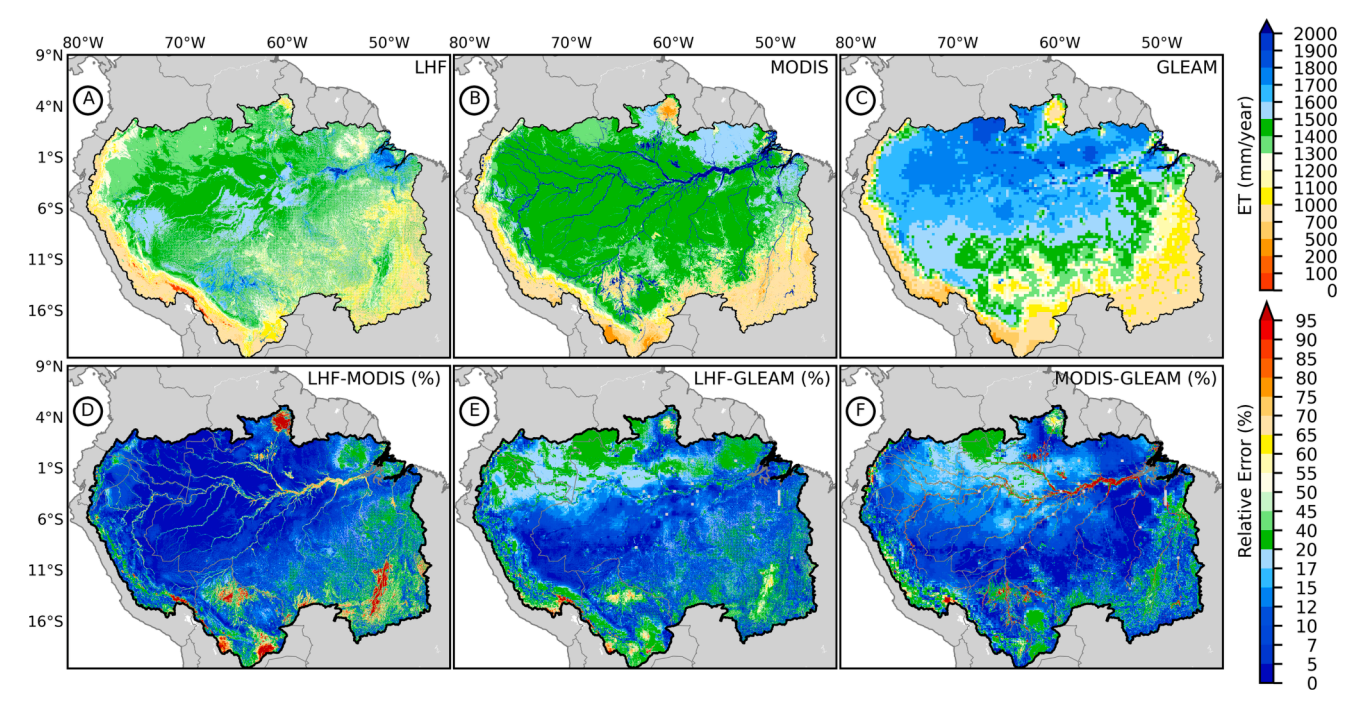


Fig. 3. Decadal mean of the spatial distribution of annual ET in the past two decades from LHF model (A), MODIS (Running et al., 2021) dataset (B), and GLEAM (Martens et al., 2017; Miralles et al., 2011) dataset (C). The relative errors (%) in LHF results compared to MODIS and GLEAM are shown in panels D and E, respectively. Panel F shows the relative difference between MODIS and GLEAM.

significant (Mann-Kendall test; 95% confidence level; markers in Fig. 4L). Examining the ARB at the basin scale, conspicuous indications of a diminishing trend are discernible across its southeastern, southern, western, and central portions which are dominantly driven by precipitation and influenced by net radiation (Fig. 4A and 4B). It is worth noting that the magnitude of this declining trend varies in correspondence with the prevailing trends in precipitation (Fig. 4G) and net radiation (Fig. 4H). In situations where precipitation has undergone a decrease and net radiation a concurrent increase, the decline in TWD level is more pronounced relative to other regions where a decreasing trend in precipitation and net radiation can be seen. In contrast, some portions within the basin exhibit an upward trend in WTD with an average slope of 44 mm/year over these regions. This ascending trend, notably observed in the northeastern extremity of the basin, can be attributed to an increase in precipitation. The expansion in positive trend in the "arc of deforestation" areas can predominantly be attributed to the reduction in ET stemming from deforestation practices (Panels D and L in Figure S4). These actions lead to a reduction in the available evaporative surfaces (substantial reduction in LAI) within these localized zones where increase in ground evaporation could not compensate for sharp reduction in transpiration (Figure S4).

A closer examination of decadal trends in WTD reveals the dominant role of precipitation while also underscoring the prominent role of net radiation in governing the dynamics of WTD at larger temporal and spatial scales (Fig. 4A, B, and F). The decadal analyses offer further insights into the aforementioned observation, particularly in light of divergent changes in precipitation and net radiation during the 2000s and 2010s (Figure S2). This phenomenon is pronounced in the northwest and northeast areas of the basin, where relatively limited deforestation has occurred. During the 2000s, groundwater storage experienced a general decline, manifesting as deeper water tables in many regions (Figure S3). A decrease in precipitation within the northwestern region of the basin was accompanied by a concurrent decline in WTD within that same geographical area (Figure S3). Further, contrasting outcomes are observed in the northeastern ARB, where increased precipitation resulted in a notably shallower WTD, where the augmenting net radiation played a key role in regulating this

mechanism. Analyzing the alterations in precipitation, net radiation, and WTD throughout the 2010s reveals a pattern that runs in contrary to the changes detailed earlier. Groundwater depth is another major modifier for WTD dynamics at large temporal and spatial scales (Fig. 4F and L). The southeastern subbasins exhibited an accelerated WTD decline in the 2000s due to reduced moisture transport into these areas (Figure S2). Here, the "dry gets drier" paradigm is evident, with regions with deeper water tables experiencing greater declines (e.g., Feng and Zhang, 2015). This trend can be attributed to reduced precipitation and infiltration, exacerbated by deforestation in certain regions (Figures S1 and S2).

The contribution of decadal changes in WTD (Fig. S3A-C) to the long-term trend (Fig. 4L) exhibits considerable spatial variations. While the decadal changes from the 1990s to the 2000s dominate the long-term trends in the northeastern ARB, the changes from the 2000s to the 2010s dictate the long-term trends more strongly along the Andes and the central-southern portions of the basin. In the southeastern ARB, the strong and significant long-term trend is a result of persistent decline in WTD during the past three decades (Fig. 4L and S3A-C), which can be further linked to a notable decline in precipitation in this region (Fig. S2A-C).

The area fraction (the proportion of the basin/subbasin area that is occupied by a particular range of WTD) of varying WTDs indicates that WTD of less than 2m is dominant across the ARB (~34% area), whereas WTD between 2 and 5m is common in ~30% of the basin (Fig. 4F and Table S1). This implies that at least 34% of the forest over the ARB is supported by groundwater during the dry season, which underscores the importance of shallow groundwater for forest resilience in the ARB. At the subbasin scale, in over 50% of the Solimoes, Japura and Negro basins WTD is shallower than 2m, suggesting an even greater groundwater role in these subbasins. In Madeira and Purus, WTD is shallower than 2m in ~30% of areas, whereas in Tocantins, Xingu, and Tapajos, such shallow groundwater is not commonly observed. Further, in Purus, Solimoes, Japura and Negro subbasins, areas with WTD within the top 5m accounts for  $\sim$ 70% while the WTD is between 2 and 5m in  $\sim$ 30% of areas. Lastly, WTD is between 5 and 10m in 10% of areas in Solimoes, Japura and Negro and 20-30% in the other subbasins.

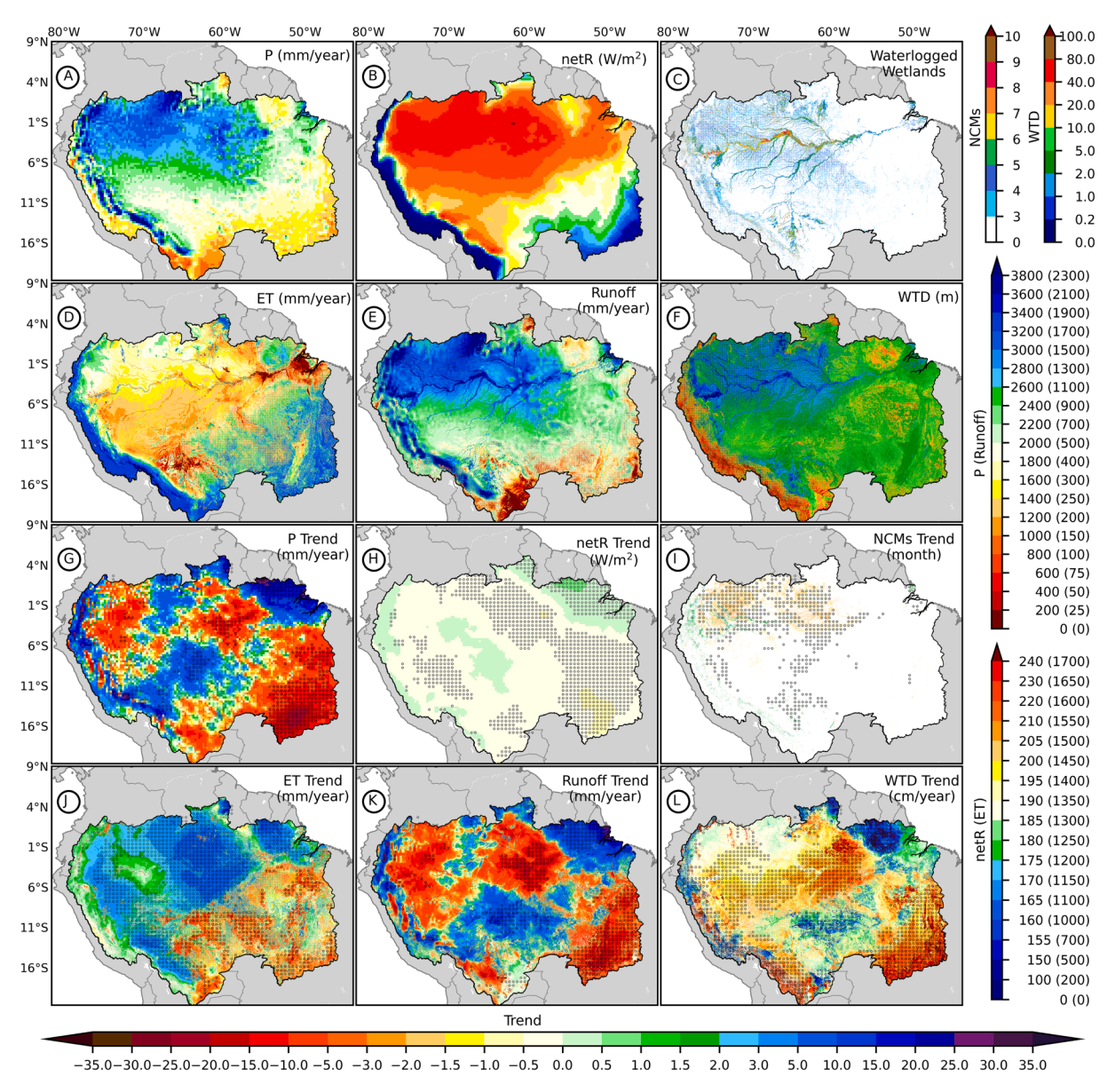


**Fig. 4.** The long-term (1992–2020) trends in the major drivers and major components of water and energy balances in the ARB over the past three decades. The long-term mean of annual precipitation, net radiation, ET, runoff, and WTD are shown in panels A, B, D, E, and F, respectively. Panel C shows waterlogged wetlands based on the number of consecutive months with WTD<0.25m. The Mann-Kendall trends and significance (markers) at 95% confidence level for precipitation, net radiation, waterlogged wetlands, ET, runoff, and WTD are shown in panels G to L, respectively.

In terms of the temporal evolution, during the 1990s, WTD was shallower than 0.25m in over 4.5% of ARB which supports water-logged wetlands (Table S2). At the subbasin scale, such shallow WTD is observed in  $\sim 10\%$  of the Solimoes, Japura, and Negro subbasins. In the Tocantins, Xingu, and Purus, WTD is mostly deeper than 0.25m. The decadal analysis shows that the area fraction of WTD shallower than 0.25m decreased by ~42% from the 1990s to the 2000s; however, it recovered by  $\sim$ 7% in the 2010s (Table S2). Over the past three decades, the area fraction of WTD<0.25m decreased by ~38%, which likely caused significant biodiversity and ecosystem loss if it passed the functional thresholds for these systems. The area fraction of WTD<2m also decreased over the ARB by  ${\sim}17\%$  from the 1990s to the 2000s, with an additional decline in the 2010s by  $\sim$ 4%. This amounts to a total decline in areas with WTD<2m by  $\sim\!\!19\%$  during the past three decades. Most of this reduction occurred in regions with WTD less than 1m. As a result, the areas with WTD less than 2m and greater than 1m increased by  $\sim$ 5% and most of this increase occurred in the Solimoes and Negro subbasins. The areas with WTD between 5 and 20m increased at the expense of decline in areas with shallower WTDs.

The analysis of the consecutive months with shallow groundwater (<0.25m; following Miguez-Macho and Fan, 2012a) shows the role of groundwater in supporting waterlogged wetlands (Fig. 4C). The following key observations can be made from this figure. First, waterlogged wetlands exhibit a predominant presence alongside the main river channels within the Amazon River, displaying notable prevalence within the Madeira, Solimoes, Japura, and Negro subbasins. Second, the waterlogged wetlands are highly dependent on high precipitation since groundwater is very shallow in these regions and groundwater buffer is relatively small. Third, a detailed temporal analysis reveals that regions experiencing continuous waterlogging for 6 to 9 months, particularly within the central and northern reaches of the basin, have witnessed a reduction of over 2 months during the past three decades (Fig. 4I). Conversely, certain waterlogged regions along the mainstem Amazon, the extended Andes region, and the Madeira subbasin, have undergone an increase of at least one additional month of waterlogging as compared to the trends three decades ago. Fourth, the decadal analysis

suggests that the waterlogged wetlands decreased by over 37% in the past three decades (Figure S3 and Table S2). The highest decline occurred in the Solimoes, Negro, Madeira and Japura, in a descending order. Fifth, these types of wetlands do not recover in a short timeframe (Figure S3). Although annual precipitation increased in the 2010s, the extent of wetlands did not change significantly. Overall, the extent of waterlogged wetlands decreased substantially across the ARB.

### 3.2.2. Dynamics of ET processes

The long-term basin-averaged ET changed with a split pattern of  $\pm 9\%$  during the past three decades. ET is more homogenously distributed within the basin's boundaries in 1990s in comparison to 2010s (Table 1), with some areas exhibiting lower ET attributable to limited net radiation (e.g., Andes; Fig. 4B) or water availability (e.g., Tocantins subbasin; Fig. 4A). Results indicate that ET exhibits strong positive (significant) trend with an average slope of ~3 mm/year over majority of the central and western ARB with a mixed signal in the eastern and southeastern regions (Fig. 4J). Again, the spatial patterns of trends are a result of spatially heterogenous changes in ET during the past three decades (Fig. S3D-F) which has been noted in the previous studies as well (Heerspink et al., 2020). Over the past two decades (2000s and 2010s), the spatial distribution of ET has undergone a noticeable shift from a relatively homogenous pattern to a distribution that is more pronounced in the central regions of the ARB (Fig. 4D). The findings suggest that the primary driver for this shift is a significant increase (decrease) in transpiration (Figure S4) resulting from climate variability (LULC change). Analyzing the longterm-mean of ET over the past three decades (Fig. 4D) reveals three distinct major regions within the ARB, each characterized by different ET characteristics. The central region of the ARB, known for its high rainfall (Fig. 4A) and dense forest cover (Figure S1), exhibits the highest rates of ET among the identified regions. In contrast, the northwestern region of the ARB displays relatively lower ET values compared to the central region, primarily due to reduced surface radiation (Figure S2) despite receiving greater precipitation than the central region (Figure S2). The southeastern region of the ARB stands out with substantially lower ET rates compared to the other regions, which can be attributed to the combined effects of deforestation and a lower rate of precipitation in this specific area (Fig. 4D, S1, and S2).

Over the northwestern region of the ARB transpiration and canopy interception loss emerge as the primary components of ET (Figures S4), whereas transpiration dominates over the central regions. Over major parts of Madeira, the majority of Tocantins and the boundaries of the southern subbasins ground evaporation stands out as the most dominant component of total ET, following transpiration. The change in ET in the 2000s is caused primarily by the change in transpiration rather than the other components (Figure S4). However, for the decrease in ET in the southern regions in 2000s, the change in ET partitioning is more complex. Over the agricultural lands in these regions ground evaporation increased, however, transpiration and canopy interception loss decreased, resulting in an overall decrease in ET with an average slope

of  $\sim$ 3.2 mm/year. Among the southern subbasins, Tocantins is different from others in that the decrease is mostly a result of decrease in ground evaporation. The changes from the 1990s to the 2000s are far more pronounced than the changes in ET from the 1990s to the 2010s. Overall, the results indicate that ground evaporation in the ARB is more sensitive to climate variability than transpiration.

Transpiration is the dominant component of ET in the ARB and canopy interception loss and ground evaporation contribute almost equally to the total ET (Table 1). A comparison of total ET over the ARB during the 1990s, 2000s, and 2010s indicates that the total ET increased, likely driven by the increase in net radiation. Moreover, transpiration contribution to total ET increased over the past three decades by  $\sim\!5\%$ , owing to a combination of climate variability (increased due to increase in surface radiation) and human impacts (decreased due to deforestation). At the subbasin scale transpiration is the dominant component of total ET, but canopy interception loss and ground evaporation do not contribute equally to total ET as on the entire ARB scale. Canopy interception loss in Purus, Solimoes, Japura and Negro is the dominant contributor to ET after transpiration, but in Tocantins, Tapajos and Madeira ground evaporation contributes most dominantly to ET after transpiration.

### 3.2.3. Dynamics of runoff and river discharge

The ARB displays two distinct regions characterized by high and low runoff, related primarily to precipitation patterns (Fig. 4A and E). The high runoff regions encompass the central, northern, western, and southwestern parts of the basin. In these areas, runoff dynamics are primarily governed by precipitation, as in these regions, the water table is relatively shallow (e.g., within 2m from the surface) (Fig. 4F). Analysis of the long-term trend of runoff over the past three decades reveals a complex interplay of increased and decreased runoff in these regions (Fig. 4K). However, the majority of these areas have experienced a decreased or relatively stable runoff and the trend in precipitation primarily explains the trend in runoff (Fig. 4G and 4K). Conversely, the low runoff regions comprise the northeastern, eastern, southern, southeastern, and certain central and western sections of the basin. In most of these regions, runoff has increased due to deforestation and cropland expansion (Fig. 4K and S1). Nevertheless, the effects of decrease in precipitation and increase in net radiation in the southeast and sought of this region counterbalance the runoff increase resulting from deforestation (Levy et al., 2018). As a result, these regions have experienced a decrease or marginal increase in runoff.

The long-term basin-averaged runoff changed with a heterogenous pattern ( $\pm 29\%$ ) over the past three decades across the ARB. Investigating the decadal analysis of the change in runoff offers more details about the long-term trend observed in runoff (Fig. S3G-I). Overall, runoff has decreased over some regions of the ARB by an average slope of  $\sim 8$  mm/year in the past three decades. The majority of this decrease occurred in the 2000s due to multiple major droughts during this period (Figs. S2 and S3G). In the 2010s, the runoff experienced an increase due to a rise in precipitation, but it could not reach the runoff levels observed

Table 1
The decadal mean of basin-averaged annual ET and its components (transpiration (Trans), canopy interception loss (CIL), and ground evaporation (GE) over the ARB and its subbasins (in mm/year).

Basin/Subbasin	1990s				2000s				2010s			
	ET	Trans	CIL	GE	ET	Trans	CIL	GE	ET	Trans	CIL	GE
Amazon	1322	623	329	370	1335	643	312	380	1343	652	302	389
Tocantins	1373	701	309	363	1337	688	273	376	1345	698	259	388
Xingu	1322	709	299	314	1299	699	271	329	1300	700	255	344
Tapajos	1323	612	279	432	1314	614	256	443	1328	624	248	456
Madeira	1211	542	124	544	1171	530	108	533	1172	536	104	532
Purus	1451	740	417	293	1472	777	388	307	1491	796	376	319
Solimoes	1334	600	444	290	1379	641	440	298	1372	636	428	308
Japura	1269	582	383	304	1316	627	371	317	1303	626	360	317
Negro	1325	596	416	313	1380	640	417	323	1408	660	414	335

in the 1990s over majority of the regions (Fig. S3H and S3I). At the subbasin scale, the Solimoes subbasin did not experience substantial changes in runoff. On the other hand, Tocantins, Xingu, and Madeira subbasins witnessed significant runoff decreases of approximately 48%, 18%, and 2%, respectively, with climate variability being the primary driver, mainly attributed to the reduction in precipitation (Figure S2). Conversely, the runoff in the Purus, Japura, Negro, and Tapajos subbasins increased by approximately 15%, 5%, 3%, and 1%, respectively. LULC change played a substantial role in these subbasins (Figure S1). Tapajos and Xingu subbasins stand out with the highest impact of LULC change, showing runoff increases of more than 5% over the past three decades. These results emphasize the combined influence of climate variability and LULC change in shaping the variability of runoff across different subbasins within the ARB.

In the 2000s river discharge in Xingu, Tapajos and major parts of Madeira remained relatively stable (Fig. S3J). Over the northeastern regions of the ARB, river discharge increased in some river portions such as in the Negro. However, over other areas of the basin, river discharge decreased substantially, especially in the downstream reaches. In the 2010s, river discharge in areas that had experienced a decrease in the 2000s, increased substantially (Fig. S3K). However, over the northeastern regions of the basin the areas that experienced an increase during the 2000s, river discharge decreased or remained unchanged. The only consistent decreasing trend over the past three decades is in the Tocantins, which can be observed primarily in the main river channels (Fig. S3L). These results indicate that river discharge in the ARB has a delayed response compared to ET and WTD. The analysis of TWS presented in the following will further corroborate this finding.

The decadal analysis of river discharge seasonality indicates that the lowest monthly river discharge (in October) decreased by  $\sim\!23\%$  during the past three decades while the highest monthly discharge (in May) increased by  $\sim\!3\%$  (Figure S5). Most of the reduction in the low flow occurred during the 2000s due to frequent droughts. In addition, the high flow in the 2000s occurred one month earlier (in April) than in the 1990s. The results imply that while the high flow recovered from the droughts during the 2000s, the low flow did not, even after a decade. Overall, this means that the dry season in the ARB is getting drier and the wet season is getting wetter. This finding complements the findings from previous studies pointing to an accelerating Amazonian hydrologic cycle (Barichivich et al., 2018; Chagas et al., 2022).

The decadal analysis at the subbasin scale indicates that Solimoes has a dominant impact on the high discharge in the mainstream of the ARB, while Tocantins and Tapajos have the least impact (Figure S5). However, none of the subbasins play a dominant role in governing the low discharge in the ARB. The timing of high flow has not changed over the past three decades and it occurs in March in Tocantins and Tapajos, in April in Madeira and Xingu, in May in Solimoes and Purus, and in June in Negro and Japura.

The analysis of the change in high discharge at the subbasin scales indicates that at all the subbasins and during the past three decades, river discharge at the outlet increased except for the Tocantins where it decreased by  $\sim\!16\%$  (Figure S5). The other change worth mentioning is  $\sim\!98\%$  increase in the discharge peak in Japura due to the increase in precipitation in the 2010s (Figure S2). The elongated shape of Japura and shallow groundwater level over the majority of the subbasin makes river discharge more responsive to the changes in precipitation than in other subbasins. Over the past three decades, river discharge in Tapajos and Madeira increased by  $\sim\!17\%$  and  $\sim\!15\%$ , respectively, due to a combination of increase in precipitation and deforestation (Figure S1 and S2). In the other subbasins, the changes in high discharge are well below 10% in comparison to the 1990s. Despite the increasing trend in high discharge among the majority of the subbasins, the low discharge decreased in all subbasins.

## 3.2.4. Dynamics of TWS

Results show that the spatial patterns of TWS remained relatively

stable, but its magnitude changed substantially during the past decades (Fig. 5A and S6). The spatial distribution of the trends in TWS anomalies closely parallels the trend observed in WTD (Fig. 5A and 4L). Nonetheless, it is noteworthy that the spatial pattern of the trend in floodwater anomalies governs the spatial pattern of TWS trend along the mainstem of the Amazon (Fig. 5D) which was reported by Pokhrel et al., (2013) as well; the contribution of water in river channels is less prominent (Fig. 5C). Overall, a decreasing trend in TWS anomalies is observed across the ARB which is largely associated with a decline in precipitation and increase in net radiation. However, some regions with an increasing trend over the "arc of deforestation", the Andes, and the northeastern areas of the basin can be observed. The increasing trend in TWS over the "arc of deforestation" is associated with decrease in ET and over the other regions with increase in precipitation and net radiation.

The decrease (increase) in the 2000s (2010s) along the mainstem of the Amazon River is associated with the fluctuations in flood water due to drought or wet periods, and as a result, no substantial trend is observed in the long-term trend (Fig. 5A) (Pokhrel et al., 2013). Tocantins subbasin experienced a decreasing trend in TWS over the past three decades due to the decline in groundwater storage which could be attributed to the reduced moisture transport into the eastern margins of ARB (Walker, 2020). Over other southern subbasins including Xingu, Tapajos and Maderia subbasins, TWS decreased from the 1900s to the 2000s and it increased from the 2000s to the 2010s. The changes in TWS over the southern subbasins are dominantly associated with the changes in groundwater storage (Fig. 5B and S6). Negro, Japura and Solimoes subbasins experienced a decrease in TWS from the 1990s to the 2000s; however, in the 2010s TWS increased in comparison to the 2000s. While flood water is the dominant component of the variations in TWS in these subbasins, groundwater component is the dominant contributor to TWS. Over the northeast region of the ARB, TWS increased substantially during the 2000s due to a large drop in WTD in comparison to the 1990s. The same region experienced a decrease in TWS from the 2000s to the 2010s. Again, groundwater is the dominant portion of TWS in this region and the variations in WTD lead to changes in TWS there. As depicted in Figure S6, the changes in TWS for the majority of regions across the ARB are governed by groundwater which confirms our hypothesis regarding the mediating role of shallow groundwater. It should be noted that in the LHF model soil moisture and groundwater compete for the same subsurface store (Pokhrel et al., 2013), thus an increase in groundwater storage would lead to a decrease in soil moisture, and vice versa.

## 3.3. Governing hydrological processes

Here, we address the second research question regarding the key factors that are governing the seasonality of the ARB at the basin and subbasin scales. In addition to many other roles, groundwater in the ARB supports streamflow and ET during the dry season. The comprehensive groundwater area fraction analysis unravels the dynamics of surface-subsurface fluxes (Fig. 6), indicating that in general WTD<5m dominantly supports river discharge (Q) and ET across the ARB. The lag time between the peaks of streamflow and ET is about one month and June-November is the driest season. During April-June groundwater (with WTD<1m) supports Q, but after June it becomes deeper with WTD<2m being the more dominant condition until early September when the hydraulic gradient decreases. As seen in the Amazon panel (Fig. 6), the increase in area fraction of 1m<WTD<2m is a result of depletion in WTD<1m that occurs around June. During the past three decades (Fig. 6), the role of groundwater to support stream discharge and ET during the dry season increased at the peak of the dry season by  $\sim$ 7% and  $\sim$ 30%, respectively. The dry season was longer ( $\sim$ 1 month) and more pronounced in the 2010s than it was two decades ago. Subsurface, river, and flood storages, on average, contribute to 69%, 26%, 5% of total TWS variability in the ARB, respectively. Subsurface storage fluctuates by  $\sim 16\%$  seasonally to mitigate surface water and ET deficits. Contribution of subsurface storage increased in the 2010s, contributing

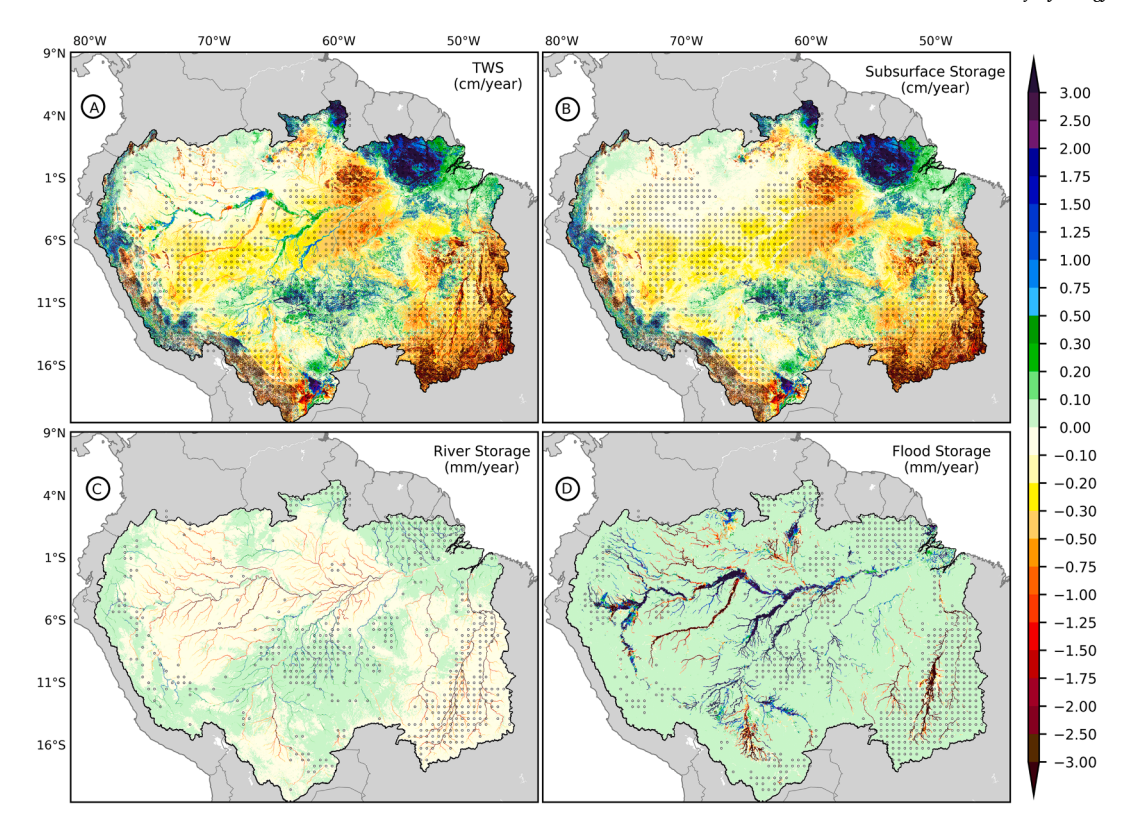


Fig. 5. Temporal (1992–2020) trend in simulated TWS anomalies (panel A) and the anomalies of its components, namely subsurface (B), river (C), and floodwater (D) stores, across the ARB. Markers indicate significant trends from Mann-Kendall test at 95% confidence level.

by more than 21% to the total storage variability than it did in the 1990s. The impacts of frequent droughts in the 2000s are evident in the surface and subsurface storages through substantial decadal changes in the timing and magnitude of peak subsurface, river and flood storages contributions in TWS variability (Fig. 6). From the 1990s to the 2000s, annual mean of floodwater contribution in TWS variability decreased by  $\sim$ 38%, and as a result, the ratio of Q to precipitation (Q/P) decreased by  $\sim$ 5%. The timing and seasonality of Q/P in the Solimoes, Madeira, Tapajos, and Purus are similar to those in the entire ARB. The substantial difference between these subbasins comes from the difference in the contribution of subsurface storages to the TWS variability. The share of subsurface storage in total TWS variability in Solimoes, Tapajos, and Purus is more pronounced than Madeira. This implies that Solimoes, Madeira, Tapajos, and Purus have a dominant impact on the seasonality of surface and subsurface fluxes in the ARB.

The seasonal cycle of ET over precipitation ratio (ET/P) and Q/P in the Tocantins overlaps almost perfectly without any noticeable lag between their peaks. This is because the Tocantins receives the lowest amount of precipitation among the ARB subbasins. Moreover, shrubland is the dominant form of LULC in the subbasin (Figure S2) and ground evaporation contributes to total ET almost equally as transpiration (Table 1). In terms of timing, E/P peak occurs in July, one month earlier than in the ARB, however, Q/P peak occurs at the same time as in the ARB (in July). Therefore, the terrestrial hydrological cycle in the Tocantins is more strongly governed by groundwater than over the entire ARB. In addition, Q seasonality in the Tocantins contributes to the high flows in the ARB and ET seasonality in Tocantins causes a longer dry period in the ARB. In the Tocantins, groundwater contribution to surface fluxes (Q and ET) begins one month earlier than in the ARB; during March-June WTD<1m supports the surface fluxes, leading to a substantial reduction in shallow groundwater storage. During June-July, 1m<WTD<2m dominantly supports the surface fluxes, and the contribution from 2m<WTD<5m begins in early August. In the Tocantins, subsurface, flood, and river storages, on average, contribute to 92%, 6%,

2% of total TWS variability, respectively. Subsurface storage fluctuates by  $\sim\!5\%$  seasonally to mitigate Q and ET deficits, experiencing an overall decadal decreasing trend. Xingu followed similar timings as in the Tocantins.

In the Negro sub-basin over 88% of the area is covered by forest, and it receives an average annual precipitation of ~3,000 mm (Fig. 4A and S1). As a result, groundwater only compensates for the Q deficit during the dry season. The dry season in the Negro (June-October) is the second shortest after Japura. The Q/P and ET/P peaks (in September and October, respectively) occur two months later in the Negro than in the ARB (Fig. 6). Therefore, Q seasonality in the Negro contributes to the amplitude of high flows in the ARB, but ET seasonality in the Negro does not contribute to the dry period in the ARB. WTD<1m supports Q during June-September. In addition, at the northern region of Negro that is covered with shrublands (Figure S1), groundwater is deeper than in the other areas in the subbasin (Fig. 4F), and it also receives 1,500 mm/year of precipitation which is substantially less than the average precipitation over the ARB (Fig. 4A). In the northern region, WTD<5m from February to October supports Q and ET (Fig. 6). In Negro, subsurface, flood, and river storages, on average, contribute to 75%, 22%, and 3% of total TWS variability, respectively. The seasonality of Q and ET and dynamics of groundwater in Japura is similar to that in Negro. However, since it is partially located in the two hemispheres, ET/P has two peaks. The first peak occurs around January and the second around September.

The ARB is dominantly energy limited where solar radiation governs ET (Fig. 4B and D). Precipitation and shortwave radiation seasonality across the ARB are out of phase from July to October, but shortwave radiation and ET are in phase throughout the year. During March-August, precipitation decreases; however, groundwater buffer prevents substantial drop in ET. These results imply that in the absence of groundwater support, and with less than  $\sim 125$  mm/month of precipitation (Amazon panel in Fig. 7), the ARB could have become water-limited over some regions.

On average, the share of transpiration, canopy and ground

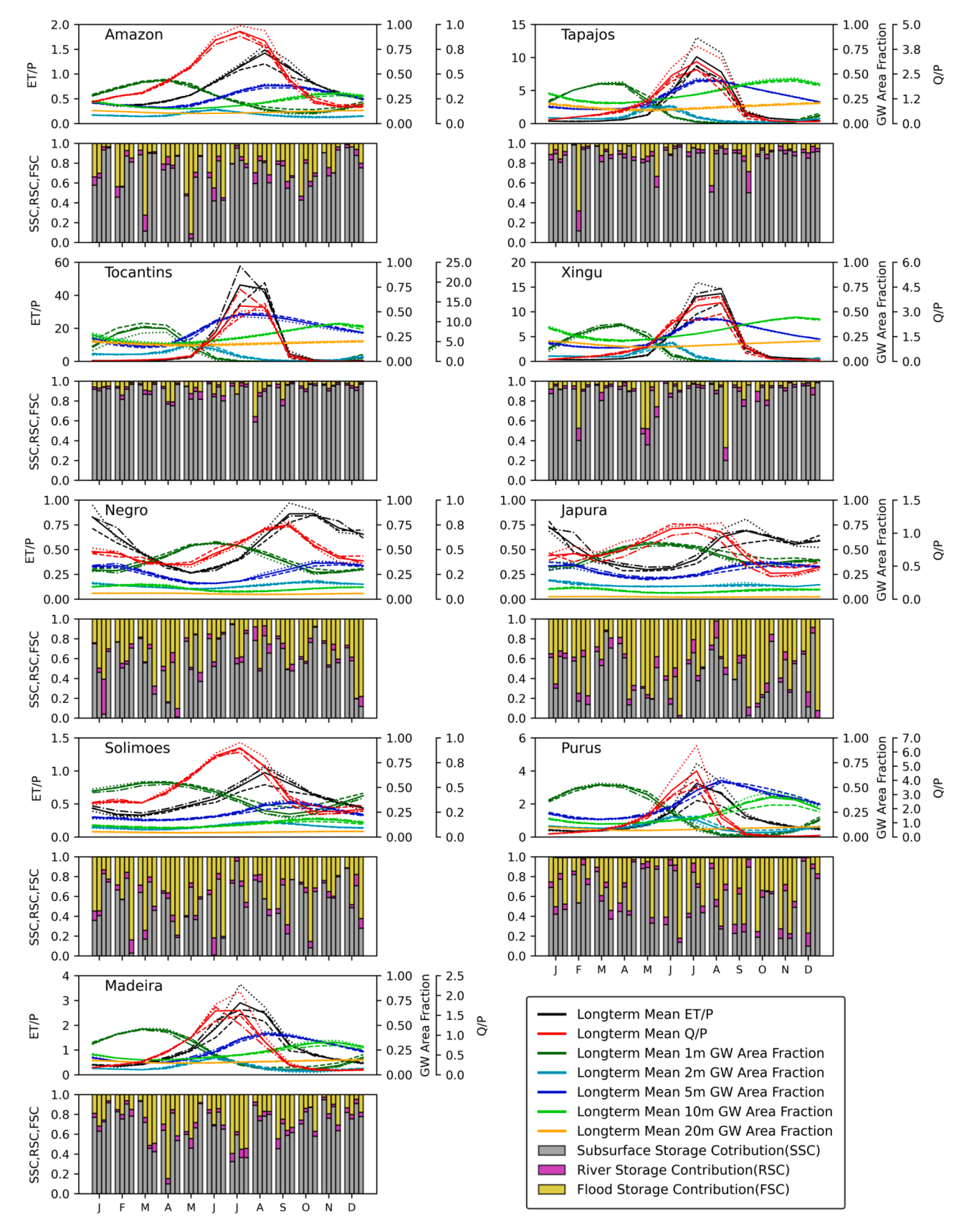


**Fig. 6.** Ratio of monthly ET (left axis) and Q (far right axis) to precipitation, and groundwater area fraction for different water table depths (right axis) for the entire ARB and its major subbasins (top panels). Solid, dashed, dotted-dashed, and dotted lines indicate the long-term mean, 1990s mean, 2000s mean, 2010s mean, respectively. Contribution of subsurface (SSC), river (RSC), and floodwater (FSC) storage components to the monthly TWS anomaly for the ARB and its subbasins (bottom panels). The first, second, third, and fourth bars for each month represent the averages for 1992–2020 (long-term), 1990s, 2000s, and 2010s, respectively.

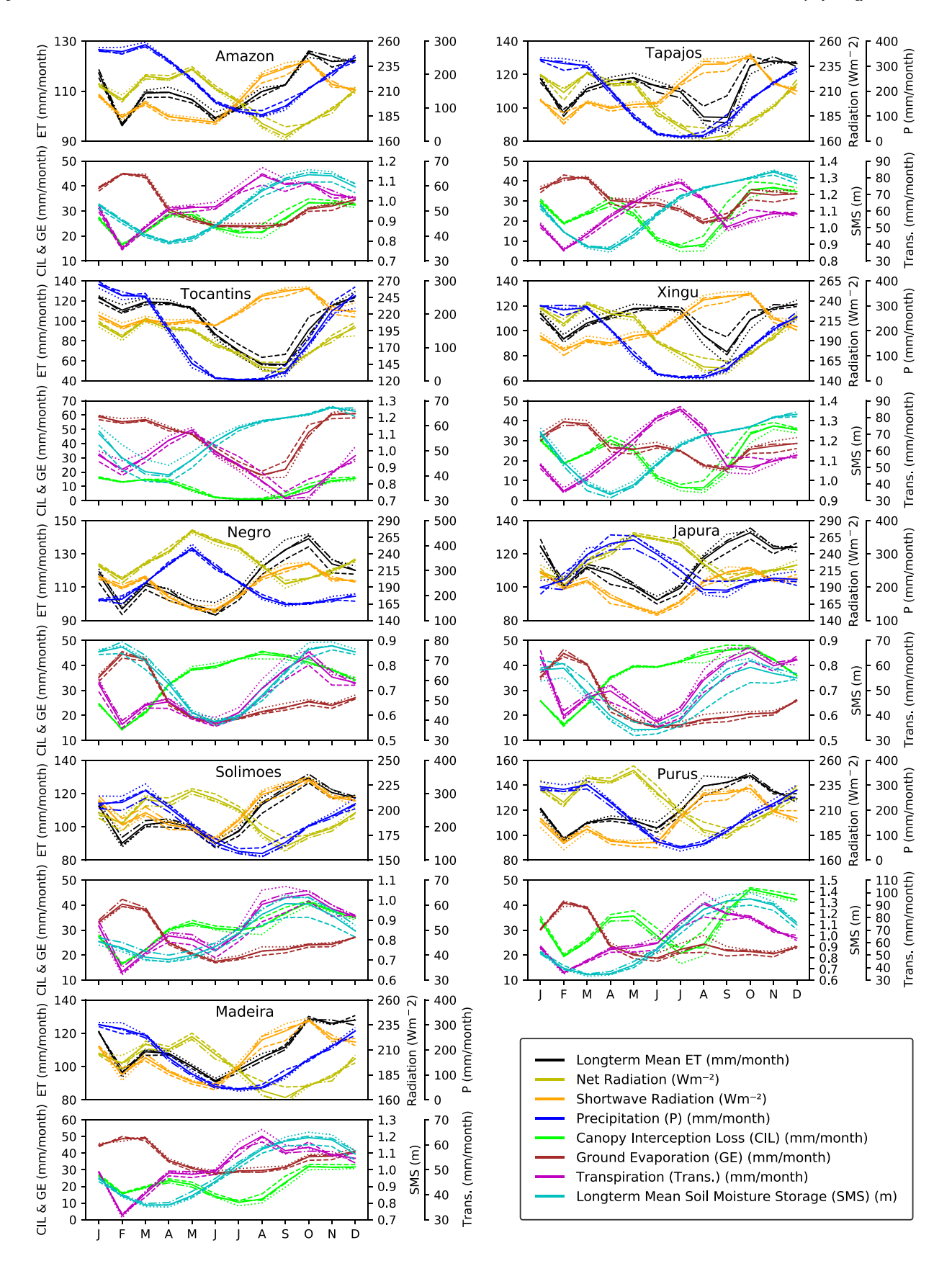


Fig. 7. Seasonality of ET over the ARB and its major subbasins. Solid, dashed, dotted-dashed, and dotted lines indicate the mean during 1992–2020 (long-term), 1990s, 2000s, and 2010s, respectively.

evaporation to total ET are ~48%, ~24% and ~28%, respectively (Table 1). June-November is the driest period, during which groundwater storage supports ET, leading to decrease (increase) in groundwater (soil moisture) storage (Fig. 7). Transpiration increases during this period while ground evaporation remains largely stable, which highlights groundwater support for ET. The decadal analysis shows that P and net radiation decreased by  $\sim 12\%$  and  $\sim 3\%$  respectively and ET remaind unchaged during June-September from the 1990s to the 2000s. Therefore, ET did not decrease substantially despite the large decline in precipitation. This again confirms the role of shallow groundwater (<5m deep) in mitigating ET deficit. The decadal analysis on ET components in the 2000s indicates that the decadal average of annual transpiration and ground evaporation increased by ~3% in comparison to the 1990s. However, the decadal average of annual canopy interception loss decreased by ~5% which is due to the substantial deforestation that happened in this decade (Figure S1). A similar trend is found in the 2010s in comparison to the 1990s; annual ET, transpiration and ground evaporation increased by ~2%, ~5%, and ~5%, respectively, whereas canopy interception loss decreased by  $\sim$ 8%.

At the subbasin scale, the seasonality of ET and its components exhibits similar hydrological behavior within three distinct subbasin groups: i) Solimoes, Madeira and Purus; ii) Tocantins, Tapajos and Xingu; and iii) Negro and Japura. The hydrological behavior observed in the first group closely mirrors that of the ARB. On average, the components, transpiration, canopy interception loss, and ground evaporation, contribute approximately 47%, 24%, and 29% to the total ET, respectively (Table 1). A decadal analysis within this group reveals substantial changes from the 1990s to the 2000s, with relatively minor fluctuations from the 2000s to the 2010s. The increase in ET within this subgroup is primarily attributed to climatic variability; however, deforestation in the Madeira has masked these increases due to climate variability, resulting in a reduced ET rate in comparison to the 1990s. In summary, over the course of the 2000s and 2010s, the decadal averaged annual ET in Solimoes and Purus subbasins exhibited an increase of  $\sim$ 3%, while Madeira experienced a decrease of  $\sim$ 3%. The increase in transpiration predominantly influenced the interdecadal variability of ET in Solimoes and Purus, whereas canopy interception loss played a dominant role in the changes observed in the Madeira subbasin.

In the second group, the share of transpiration, canopy interception loss, and ground evaporation to total ET is  $\sim$ 50%,  $\sim$ 18% and  $\sim$ 31%, respectively (Table 1). Consequently, ground evaporation plays a more prominent role in governing the seasonal dynamics of ET in this group compared to the first group (Fig. 7). A decadal analysis of this group elucidates the factors contributing to the decrease in ET during the 2000s and 2010s when contrasted with the 1990s. On average, ET in Tocantins, Tapajos and Xingu decreased by over 10% in August (driest month) from the 2010s to the 1990s. While all components of ET contribute to this decrease, the majority of that is due to over 34% decrease in canopy interception loss. It is noteworthy that canopy interception loss evaporation in these subbasins is primarily driven by the evaporation from croplands and shrublands. Specifically, croplands cover approximately 28%, 21%, and 13% of the respective areas in Tocantins, Tapajos, and Xingu, while shrublands encompass around 57%, 7%, and 8% of these regions. In contrast, in the third group of subbasins, Negro and Japura, the contributions of transpiration, canopy interception loss, and ground evaporation to the total ET are approximately 46%, 32%, and 22%, respectively. Over the 2000s and 2010s, ET increased by  ${\sim}6\%$  and  ${\sim}3\%$  in Negro and Japura, respectively, with the change in transpiration exerting a dominant influence on this direction of change.

### 3.4. Early/Late warning signals

Early and late warning signals play a pivotal role in monitoring and responding to hydrological changes within the ARB. This section addresses the third research question, providing insights into the implications of these signals, emphasizing their importance in understanding hydrological dynamics and enabling effective management strategies. As shown in section 3.3, WTD <5m has a dominant impact on the seasonality of surface fluxes at the basin and subbasin scales and it largely mitigates the impacts of climate variability and LULC change on ET and river discharge (Fig. 3). However, the mitigation impact of groundwater for ET is more limited than river discharge.

Assessing hydrological changes within the ARB requires a nuanced understanding that extends beyond standard hydrologic indicators such as river discharge. Our findings underscore the limited utility of river discharge as a standalone indicator, given its strong dependence on groundwater dynamics (Fig. 6). Providing a more nuanced perspective, alterations in ET distribution serve as valuable precursors of hydrological shifts (Table 1). While groundwater largely supports ET during the dry season, shifts in ET patterns provide valuable early indications of hydrological changes. Notably, in the deforested regions, increased ground evaporation partially compensates for reduced transpiration due to diminished LAI. Integrating remote sensing data and harnessing computational advancements can enhance the monitoring of ET dynamics by reducing the latency of distributed hydrological models.

Spatial patterns of shallow groundwater area fractions (Fig. 4F) offer another layer of early indicators. These indicators spotlight regions undergoing variations in hydrological processes, directing immediate attention, and enabling prompt management interventions. However, observational WTD datasets are notably absent in the ARB, impeding comprehensive management strategies. While the establishment of a monitoring well network within the top 5m of the land surface remains crucial, this study demonstrates (see section 3.2.4) the potential utility of GRACE data as a proxy for monitoring WTD dynamics. It is, nevertheless, important to acknowledge that while GRACE offers insights, its uncertainties and coarse resolution, render it unreliable for local and finer-scale monitoring.

Late warning signals, primarily rooted in TWS changes, intricately reflect alterations in floodwater and groundwater dynamics (Fig. 5). Understanding how climate variability and human activities influence TWS alterations is pivotal for devising adaptable management strategies. By embracing both early and late warning signals, hydrological monitoring and management strategies can be holistically designed to mitigate the impact of hydrological fluctuations. In essence, the interplay of early and late warning signals significantly contributes to our understanding of hydrological transformations within the ARB. These signals, specifically derived from ET distribution, spatial groundwater patterns, and TWS shifts, could collectively pave pathways for a more comprehensive and effective hydrological monitoring and management framework. This framework, in turn, empowers stakeholders to anticipate, respond to, and alleviate the impacts of hydrological changes in a proactive and informed manner.

### 3.5. Hydrological implications for forest management

The analysis of groundwater area fraction revealed that waterlogged wetlands (i.e., areas with WTD<0.25m) are located mostly along the main channel of the Amazon River which are not permanently flooded and are supported by rather shallow groundwater as noted by Miguez-Macho and Fan (2012a) as well. The variation in the extent of these wetlands is strongly governed by precipitation because groundwater is very shallow in waterlogged regions. As such, large-scale LULC change in the ARB, which could cause substantial change in precipitation (through change in moisture recycling or shift in the precipitation pattern) should be avoided (Nobre et al., 2016). The extent of these wetlands should be considered as the first criterion in any management/development practices since any shift in precipitation pattern will impact the waterlogged wetlands and they are a rich niche for ARB biodiversity (Duponchelle et al., 2021). The second design criterion could be the area fraction of WTDs of up to 5m. As indicated by the comprehensive analysis of the area fraction of WTDs, groundwater

sustains surface fluxes during the dry season. Therefore, the management/development practices could support this process by preserving the extent of WTD area fraction and tree species with rooting depth of more than 5m. In cases where a change in land use is unavoidable, WTD area fraction could be maintained within some thresholds that do not alter various impacted processes discussed in the results section. It is worth noting that the seasonal dynamics of groundwater area fraction beyond the thresholds can cause seasonal drought and waterlogging stress to favor the condition for other alternatives state at least at local scales (Fan et al., 2017; Hirota et al., 2011; Khanna et al., 2017; Lovejoy and Nobre, 2019; Mattos et al., 2023; Staal et al., 2020, 2018; Staver et al., 2011).

The third management criterion could be the lag time between the peak of Q/P and ET/P. As shown in the WTD fraction area analysis at the basin scale (Fig. 4) the lag time is the key in sustaining the rainforest from tipping into savanna. Therefore, it is crucial to sustain the lag time of Q/P peak to which occurs around two months earlier than ET/P peak in the subbasins with intensive land use. The fourth management criterion could be the spatial distribution of ET. Management practices that result in a more homogenous distribution of ET across the ARB could be beneficial. As shown in the results, the deforestation across the "arc of deforestation" caused a shift in ET pattern, and higher contribution of forested regions will increase the chance of forest degradation and dieback (Cox et al., 2004; Zemp et al., 2017). Similar strategies can be applied to the subbasins with similar hydrological behavior. The analysis of groundwater area fraction in conjunction with seasonality of ET/ P, Q/P, and TWS components showed that Tocantins, Tapajos and Xingu have similar hydrological responses. Furthermore, hydrologically speaking, the Solimoes, Madeira, and Purus can be categorized into one group, while the Negro and Japura subbasins can be considered in another distinct group.

The trend and decadal analyses showed that ET is one of the earliest key hydrological variables which responds to climate variability and anthropogenic impacts by shifting from a uniform to a forest concentrated pattern. This is because over tropical forests, transpiration is the dominant contributor to total ET, as a results, over the deforested regions ET reduces substantionaly. Therefore, the substantial change in ET pattern can be taken as an early warning signal. In addition, we showed how WTD area fractions change seasonally and at the interdecadal scale to mitigate the changes in ET and river discharge. The trend analysis on groundwater storage indicates that there is a decreasing trend in the storage, implying that groundwater storage can be taken as another warning signal for hydrological alteration over the ARB.

Overall, the results showed that the status of groundwater shallow area fraction in conjunction with the spatial distribution of ET can be taken as a proxy for assessing the future of management practices. The spatial distribution of ET and the dynamics of shallow groundwater area fraction can serve as early warning signals, meanwhile, the changes primarily rooted in TWS alterations should be monitored as late indicators of hydrological shifts in the ARB. However, in the deforested areas ET is highly impacted by climate variability since ground evaporation is the dominant contributor to the total ET after transpiration. For example, in Tocantins, ground evaporation contributes to over 43% of total ET, therefore, ET would indicate the changes that occur locally and under climate variability rather than due to human disturbances. The comprehensive area fraction analysis of groundwater showed that WTDs of up to 5m are the governing hydrological attributes of the ARB. The WTD<5m fulfills a wide range of functions and supports ET and river discharge across the ARB. However, there is no comprehensive observational dataset of WTD available in the ARB, even though such a dataset is crucial for management, deploying policies and future management practices in the ARB. Therefore, it is important to develop a network of monitoring wells especially in the first 5m from the land surface, however, as shown in this study (see section 3.2) GRACE data could be used as a proxy, but the uncertainties and coarse resolution of GRACE would not provide a reliable monitoring at local and finer scales.

#### 4. Conclusions

Dominant terrestrial hydrological processes are investigated at basin and subbasin scales based on three decades of hydrological variability and LULC change across the ARB. The results of comprehensive groundwater area fraction analysis suggested that shallow groundwater (<5m) is the dominant attribute of the ARB which strongly modulates the dynamics of surface-subsurface fluxes at basin and subbasin scales during the dry season. The results of area fraction of varying WTDs indicate that WTD<2m is prevalent at  $\sim$ 34% of the basin area, whereas WTD between 2 and 5m is common at  $\sim$ 30% of the basin. This implies that at least 34% of the Amazonian Forest is supported by groundwater during the dry season. The area fraction of WTD<2m decreased by ~19% during the past three decades. Most of this reduction occurred in regions with WTD less than 1m. As a result, the areas with WTD less than 2m and greater than 1m increased by  $\sim$ 5% and most of this increase occurred in the Solimoes and Negro subbasins. The areas with WTD between 5 and 20m increased at the expense of decline in areas with shallower WTDs. Therefore, forest management practices in the ARB, which may alter WTD, should ensure that the resultant WTD is able to support ET and river discharge through the processes discussed in the results section.

WTD<0.25m supports waterlogged wetlands at ~4.5% of the area of the ARB and up to 10% in Solimoes, Japura, and Negro subbasins. These types of wetlands are not flooded and highly dependent on precipitation to sustain their extent. The trend analysis showed a decreasing trend in the extent of the waterlogged wetlands (by  $\sim$ 37%). The impacts on the waterlogged wetlands should be considered in the management policies to avoid the unintended consequences which may disrupt the roles of these wetlands. The waterlogged wetlands are very susceptible to largescale changes in LULC and are playing an important role in sustaining the biodiversity of the ARB. The lag time between the seasonal peak of ET and river discharge is a key mechanism sustaining the rainforest from tipping into savanna. The management practices should improve the lag time in ways that the peak of discharge occurs around two months earlier than the peak of ET in the dry season. Further, the decadal analysis showed that ecohydrological processes that depend on shallow groundwater are more susceptible to climate and human factors than those dependent on deeper groundwater processes and they lose their functionality due to decrease in precipitation sooner.

The long-term basin-averaged ET changed with a split pattern of  $\pm 9\%$  with transpiration being the dominant contributor (~49%) to total ET in the past three decades. The contribution of transpiration (~4% increase), canopy (~2% increase) and ground evaporation (~6% increase) evolved dramatically in response to deforestation. As ET increased over the forested regions due to climate variability impacts and it decreased over deforested regions due to a combination of climate variability and deforestation impacts; the spatial distribution of ET shifted from a homogenous distribution to a more intense ET in the central region of the ARB. The shift in ET intensity distribution can lead to further forest degradation and dieback in the forested areas where the forest contributes more than it used to do three decades ago. WTD ( $\pm 19\%$ ) and runoff ( $\pm 29\%$ ) changed with a heterogenous patterns across the ARB. Analyzing river discharge confirms the crucial buffering role of groundwater. The results of this analysis imply that while the high flow recovered from the droughts during the 2000s, the low flow did not, even after a decade. Overall, this means that the dry season in the ARB is getting drier and the wet season is getting wetter, pointing to an accelerating hydrologic cycle. The ARB is dominantly energy limited, however, our results imply that in the absence of groundwater support, and with less than ~125 mm/month of precipitation, the ARB could have become water-limited over some regions of the basin. These results also indicate that river discharge in the ARB has a delayed response to the changes in the basin compared to ET and WTD. The only consistent decreasing trend over the past three decades, which is observed in the main river channels, is in the Tocantins. Terrestrial water storage (TWS)

decreased (increased) in the 2000s (2010s) compared to that in the 1990s. The results showed that the dominant role of subsurface storage in contributing into TWS dynamics has intensified in the past three decades. Although groundwater is the dominant contributor to total TWS, the dynamics of TWS over the regions along major river channels are controlled by flood water since groundwater is relatively shallow in these regions. ET is likely to be impacted more by climate change and variability than shallow groundwater (<5m deep), therefore, groundwater storage needs to be monitored as the primary indicator of the system status in forest restoration designs. The spatial distribution of groundwater area fractions and ET can be monitored as early warning signals and the changes in TWS as a late warning signal of the changes that are occurring in the terrestrial hydrological cycle in the ARB.

The spatial resolution and temporal period of the simulations are two of the limitations of this study. The improvement of the model resolution might assist in defining some design criteria in the headwater streams which are rich instream physical habitats. However, due to the coarse input data resolution and high computational costs, it was not feasible at the time of conducting the simulations for this research to do the simulations at finer resolution than one arcminute and it is one of the limitations of this study. The ESA land cover/land use data is not available for the entire ARB before 1992. Covering the periods before 1992 could provide more insight into what the natural states of the hydrological system in the ARB were. However, since this study focused on the hydrological processes, the use of such extended simulations would not alter the key findings. Moreover, the thresholds of ET and WTD change need further research using coupled land surface and atmospheric models and by developing a wide range of scenarios which is out of the scope of this study. In sum, this study provided crucial insights on the dominant terrestrial hydrological processes in the ARB to inform forest management practices.

### CRediT authorship contribution statement

Omid Bagheri: Conceptualization, Methodology, Formal analysis, Investigation, Visualization, Data curation, Validation, Writing – original draft, Writing – review & editing. Yadu Pokhrel: Conceptualization, Funding acquisition, Investigation, Methodology, Project administration, Resources, Writing – review & editing, Supervision. Nathan Moore: Methodology, Writing – review & editing. Mantha S. Phanikumar: Methodology, Writing – review & editing.

## **Declaration of Competing Interest**

The authors declare the following financial interests/personal relationships which may be considered as potential competing interests: Omid Bagheri reports financial support was provided by National Science Foundation. Omid Bagheri reports equipment, drugs, or supplies was provided by NCAR Computational and Information Systems Laboratory. Yadu Pokhrel reports financial support was provided by National Science Foundation. Nathan Moore reports financial support was provided by National Science Foundation.

## Data availability

All input data sets used in the analyses are publicly available from the cited references. Processed data required to reproduce the figures will be made available upon request through NCAR's Computational and Information System Laboratory or HydroShare by the Consortium of Universities for the Advancement of Hydrologic Science Inc. (CUAHSI).

### Acknowledgments

We acknowledge the funding from the National Science Foundation (CAREER, Award #1752729 and INFEWS, Award #1639115). Model simulations were conducted at Cheyenne (https://doi.org/10.5065/

D6RX99HX) provided by NCAR's Computational and Information Systems Laboratory sponsored by the National Science Foundation. None of these agencies or following funding sources should be held responsible for the views herein. They are the sole responsibility of the authors. The authors thank the technical insights of Suyog Chaudhari and Mohammad Hassan Badizad in Python scripting to produce some of the figures in this study.

### Appendix A. Supplementary data

Supplementary data to this article can be found online at https://doi.org/10.1016/j.jhydrol.2023.130312.

#### References

- Aragão, L.C.E.O., 2012. The rainforest's rain pump. Nature 489, 217–218.
- Aragão, L.E.O.C., Poulter, B., Barlow, J.B., Anderson, L.O., Malhi, Y., Saatchi, S., Phillips, O.L., Gloor, E., 2014. Environmental change and the carbon balance of Amazonian forests. Biol. Rev. 89, 913–931. https://doi.org/10.1111/brv.12088.
- Aragão, L.E.O.C., Anderson, L.O., Fonseca, M.G., Rosan, T.M., Vedovato, L.B., Wagner, F. H., Silva, C.V.J., Junior, C.H.L.S., Arai, E., Aguiar, A.P., Barlow, J., Berenguer, E., Deeter, M.N., Domingues, L.G., Gatti, L., Gloor, M., Malhi, Y., Marengo, J.A., Miller, J.B., Phillips, O.L., Saatchi, S., 2018. 21st Century drought-related fires counteract the decline of Amazon deforestation carbon emissions. Nat. Commun. 9, 1–12. https://www.nature.com/articles/s41467-017-02771-v.
- Arvor, D., Funatsu, B.M., Michot, V., Dubreui, V., 2017. Monitoring rainfall patterns in the southern amazon with PERSIANN-CDR data: Long-term characteristics and trends. Remote Sens. 9, 889. https://doi.org/10.3390/rs9090889.
- Bagley, J.E., Desai, A.R., Harding, K.J., Snyder, P.K., Foley, J.A., 2014. Drought and deforestation: Has land cover change influenced recent precipitation extremes in the Amazon? J. Clim. 27, 345–361. https://doi.org/10.1175/JCLI-D-12-00369.1.
- Barichivich, J., Gloor, E., Peylin, P., Brienen, R.J.W., Schöngart, J., Espinoza, J.C., Pattnayak, K.C., 2018. Recent intensification of Amazon flooding extremes driven by strengthened Walker circulation. Sci. Adv. 4, eaat8785. https://www.science.org/do i/full/10.1126/sciadv.aat8785.
- Barkhordarian, A., Saatchi, S.S., Behrangi, A., Loikith, P.C., Mechoso, C.R., 2019. A Recent Systematic Increase in Vapor Pressure Deficit over Tropical South America. Sci. Rep. 9, 1–12. https://doi.org/10.1038/s41598-019-51857-8.
- Bates, P.D., Horritt, M.S., Fewtrell, T.J., 2010. A simple inertial formulation of the shallow water equations for efficient two-dimensional flood inundation modelling. J. Hydrol. 387, 33–45. https://doi.org/10.1016/j.jhydrol.2010.03.027.
- Beven, K.J., Kirkby, M.J., 1979. A physically based, variable contributing area model of basin hydrology. Hydrol. Sci. Bull. 24, 43–69. https://doi.org/10.1080/ 02626667909491834.
- Brown, E., Johansen, I.C., Bortoleto, A.P., Pokhrel, Y., Chaudhari, S., Cak, A., Sulaeman, S., Castro-Diaz, L., Lopez, M.C., Mayer, A., Walgren, J., Müller, N., Moran, E., 2022. Feasibility of hybrid in-stream generator—photovoltaic systems for Amazonian off-grid communities. PNAS Nexus 1, pgac077. https://doi.org/
- Bullock, E.L., Woodcock, C.E., Souza, C., Olofsson, P., 2020. Satellite-based estimates reveal widespread forest degradation in the Amazon. Glob. Chang. Biol. 26, 2956–2969. https://doi.org/10.1111/gcb.15029.
- Chagas, V.B.P., Chaffe, P.L.B., Blöschl, G., 2022. Climate and land management accelerate the Brazilian water cycle. Nat. Commun. 13, 5136. https://www.nature.com/articles/s41467.023-32580.x
- Chaudhari, S., Pokhrel, Y., 2022. Alteration of River Flow and Flood Dynamics by Existing and Planned Hydropower Dams in the Amazon River Basin. Water Resour. Res. 58 https://doi.org/10.1029/2021WR030555.
- Chaudhari, S., Felfelani, F., Shin, S., Pokhrel, Y., 2018. Climate and anthropogenic contributions to the desiccation of the second largest saline lake in the twentieth century. J. Hydrol. 560, 342–353. https://doi.org/10.1016/j.jhydrol.2018.03.034.
- Chaudhari, S., Pokhrel, Y., Moran, E., Miguez-Macho, G., 2019. Multi-decadal hydrologic change and variability in the Amazon River basin: Understanding terrestrial water storage variations and drought characteristics. Hydrol. Earth Syst. Sci. 23, 2841–2862. https://doi.org/10.5194/hess-23-2841-2019.
- Chaudhari, S., Brown, E., Quispe-Abad, R., Moran, E., Müller, N., Pokhrel, Y., 2021. Instream turbines for rethinking hydropower development in the Amazon basin. Nat. Sustain. 4, 680–687. https://doi.org/10.1038/s41893-021-00712-8.
- Clark, M.P., Fan, Y., Lawrence, D.M., Adam, J.C., Bolster, D., Gochis, D.J., Hooper, R.P., Kumar, M., Leung, L.R., Mackay, D.S., Maxwell, R.M., Shen, C., Swenson, S.C., Zeng, X., 2015. Improving the representation of hydrologic processes in Earth System Models. Water Resour. Res. 51, 5929–5956. https://doi.org/10.1002/2015WR017096.
- Costa, M.H., Foley, J.A., 1999. Trends in the hydrologic cycle of the Amazon basin. J. Geophys. Res. Atmos. 104, 14189–14198. https://doi.org/10.1029/1998JD200126.
- Costa, M.H., Pires, G.F., 2010. Effects of Amazon and Central Brazil deforestation scenarios on the duration of the dry season in the arc of deforestation. Int. J. Climatol. 30, 1970–1979. https://doi.org/10.1002/joc.2048.
- Costa, M.H., Yanagi, S.N.M., Souza, P.J.O.P., Ribeiro, Á., Rocha, E.J.P., 2007. Climate change in Amazonia caused by soybean cropland expansion, as compared to caused

- by pastureland expansion. Geophys. Res. Lett. 34 https://doi.org/10.1029/
- Cox, P.M., Betts, R.A., Collins, M., Harris, P.P., Huntingford, C., Jones, C.D., 2004. Amazonian forest dieback under climate-carbon cycle projections for the 21st century. Theor. Appl. Climatol. 78, 137–156. https://doi.org/10.1007/s00704-004-0040-4
- Davidson, E.A., De Araüjo, A.C., Artaxo, P., Balch, J.K., Brown, I.F., Mercedes, M.M., Coe, M.T., Defries, R.S., Keller, M., Longo, M., Munger, J.W., Schroeder, W., Soares-Filho, B.S., Souza, C.M., Wofsy, S.C., 2012. The Amazon basin in transition. Nature 481, 321–328. https://doi.org/10.1038/nature10717.
- De Paiva, R.C.D., Buarque, D.C., Collischonn, W., Bonnet, M., Frappart, F., Calmant, S., Bulhões Mendes, C.A., 2013. Large-scale hydrologic and hydrodynamic modeling of the Amazon River basin. Water Resour. Res. 49, 1226–1243.
- Duponchelle, F., Isaac, V.J., Da Costa, R., Doria, C., Van Damme, P.A., Herrera-R, G.A., Anderson, E.P., Cruz, R.E.A., Hauser, M., Hermann, T.W., Agudelo, E., Bonilla-Castillo, C., Barthem, R., Freitas, C.E.C., García-Dávila, C., García-Vasquez, A., Renno, J.F., Castello, L., 2021. Conservation of migratory fishes in the Amazon basin. Aquat. Conserv. Mar. Freshw. Ecosyst. 31, 1087–1105. https://doi.org/10.1002/apr.3550
- Eltahir, E.A.B., Bras, R.L., 1994. Precipitation recycling in the Amazon basin. Q. J. R. Meteorol. Soc. 120, 861–880. https://doi.org/10.1002/qj.49712051806.
- Esquivel-Muelbert, A., Baker, T.R., Dexter, K.G., Lewis, S.L., Brienen, R.J.W., Feldpausch, T.R., Lloyd, J., Monteagudo-Mendoza, A., Arroyo, L., Álvarez-Dávila, E., 2019. Compositional response of Amazon forests to climate change. Glob. Chang. Biol. 25, 39–56
- Fan, Y., Li, H., Miguez-Macho, G., 2013. Global patterns of groundwater table depth. Science 80-.). 339, 940–943. https://doi.org/10.1126/science.1229881.
- Fan, Y., Miguez-Macho, G., 2010. Potential groundwater contribution to Amazon evapotranspiration. Hydrol. Earth Syst. Sci. 14, 2039–2056. https://doi.org/ 10.5194/hess-14-2039-2010.
- Fan, Y., Miguez-Macho, G., Jobbágy, E.G., Jackson, R.B., Otero-Casal, C., 2017. Hydrologic regulation of plant rooting depth. PNAS 114, 10572–10577. https://doi.org/10.1073/pnas.1712381114.
- Fassoni-Andrade, A.C., Fleischmann, A.S., Papa, F., de Paiva, R.C.D., Wongchuig, S., Melack, J.M., Moreira, A.A., Paris, A., Ruhoff, A., Barbosa, C., Maciel, D.A., Novo, E., Durand, F., Frappart, F., Aires, F., Abrahão, G.M., Ferreira-Ferreira, J., Espinoza, J. C., Laipelt, L., Costa, M.H., Espinoza-Villar, R., Calmant, S., Pellet, V., 2021. Amazon Hydrology From Space: Scientific Advances and Future Challenges. Rev. Geophys. 59 https://doi.org/10.1029/2020RG000728.
- Fearnside, P.M., 2000. Global warming and tropical land-use change: greenhouse gas emissions from biomass burning, decomposition and soils in forest conversion, shifting cultivation and secondary vegetation. Clim. Change 46 (1–2), 115–158. https://link.springer.com/article/10.1023/A:1005569915357.
- Felfelani, F., Wada, Y., Longuevergne, L., Pokhrel, Y.N., 2017. Natural and humaninduced terrestrial water storage change: A global analysis using hydrological models and GRACE. J. Hydrol. 553, 105–118. https://doi.org/10.1016/j. jhydrol.2017.07.048.
- Feng, H., Zhang, M., 2015. Global land moisture trends: drier in dry and wetter in wet over land. Sci. Rep. 5 (1), 18018. https://www.nature.com/articles/srep18018.
- Foley, J.A., DeFries, R., Asner, G.P., Barford, C., Bonan, G., Carpenter, S.R., Chapin, F.S., Coe, M.T., Daily, G.C., Gibbs, H.K., Helkowski, J.H., Holloway, T., Howard, E.A., Kucharik, C.J., Monfreda, C., Patz, J.A., Prentice, I.C., Ramankutty, N., Snyder, P.K., 2005. Global consequences of land use. Science (80-.). 309, 570–574. https://doi.org/10.1126/science.1111772.
- Frappart, F., Papa, F., Güntner, A., Tomasella, J., Pfeffer, J., Ramillien, G., Emilio, T., Schietti, J., Seoane, L., da Silva Carvalho, J., 2019. The spatio-temporal variability of groundwater storage in the Amazon River Basin. Adv. Water Resour. 124, 41–52.
- Fu, R., Yin, L., Li, W., Arias, P.A., Dickinson, R.E., Huang, L., Chakraborty, S., Fernandes, K., Liebmann, B., Fisher, R., Myneni, R.B., 2013. Increased dry-season length over southern Amazonia in recent decades and its implication for future climate projection. PNAS 110, 18110–18115. https://doi.org/10.1073/ pnas.1302584110.
- Gash, J.H.C., 1979. An analytical model of rainfall interception by forests. Q. J. R. Meteorol. Soc. 105, 43–55. https://rmets.onlinelibrary.wiley.com/doi/abs/10. 1002/qj.49710544304.
- Getirana, A.C.V., Boone, A., Yamazaki, D., Decharme, B., Papa, F., Mognard, N., 2012. The hydrological modeling and analysis platform (HyMAP): Evaluation in the Amazon basin. J. Hydrometeorol. 13, 1641–1665. https://journals.ametsoc.org/vie w/journals/hydr/13/6/jhm-d-12-021\_1.xml.
- Guan, K., Pan, M., Li, H., Wolf, A., Wu, J., Medvigy, D., Caylor, K.K., Sheffield, J., Wood, E.F., Malhi, Y., Liang, M., Kimball, J.S., Saleska, S.R., Berry, J., Joiner, J., Lyapustin, A.I., 2015. Photosynthetic seasonality of global tropical forests constrained by hydroclimate. Nat. Geosci. 8, 284–289. https://doi.org/10.1038/ngeo2382.
- Heerspink, B.P., Kendall, A.D., Coe, M.T., Hyndman, D.W., 2020. Trends in streamflow, evapotranspiration, and groundwater storage across the Amazon Basin linked to changing precipitation and land cover. J. Hydrol.: Reg. Stud. 32, 100755 https://doi.org/10.1016/j.ejrh.2020.100755.
- Hersbach, H., B, B., P, B., S, H., A, H., J, M., J, N., C, P., R, R., D, S., A, S., 2020. The ERA5 global reanalysis. Q. J. R. Meteorol. Soc. 146, 1999–2049.
- Hirota, M., Holmgren, M., Van Nes, E.H., Scheffer, M., 2011. Global resilience of tropical forest and savanna to critical transitions. Science (80-.) 334, 232–235.
- Hoek van Dijke, A.J., Herold, M., Mallick, K., Benedict, I., Machwitz, M., Schlerf, M., Pranindita, A., Theeuwen, J.J.E., Bastin, J.F., Teuling, A.J., 2022. Shifts in regional water availability due to global tree restoration. Nat. Geosci. 15, 363–368. https:// doi.org/10.1038/s41561-022-00935-0.

- Kendall, M.G., 1948. Rank correlation methods.
- Khanna, J., Medvigy, D., Fueglistaler, S., Walko, R., 2017. Regional dry-season climate changes due to three decades of Amazonian deforestation. Nat. Clim. Chang. 7, 200–204. https://doi.org/10.1038/nclimate3226.
- Laurance, W.F., Cochrane, M.A., Bergen, S., Fearnside, P.M., Delamônica, P., Barber, C., D'Angelo, S., Fernandes, T., 2001. The future of the Brazilian Amazon. Science (80-.) 291, 438–439. https://doi.org/10.1126/science.291.5503.438.
- Laurance, W.F., Lovejoy, T.E., Vasconcelos, H.L., Bruna, E.M., Didham, R.K., Stouffer, P. C., Gascon, C., Bierregaard, R.O., Laurance, S.G., Sampaio, E., 2002. Ecosystem decay of Amazonian forest fragments: A 22-year investigation. Conserv. Biol. 16, 605–618. https://doi.org/10.1046/j.1523-1739.2002.01025.x.
- Lavagnini, I., Badocco, D., Pastore, P., Magno, F., 2011. Theil-Sen nonparametric regression technique on univariate calibration, inverse regression and detection limits. Talanta 87, 180–188.
- Lawrence, D.M., Fisher, R.A., Koven, C.D., Oleson, K.W., Swenson, S.C., Bonan, G.,
  Collier, N., Ghimire, B., van Kampenhout, L., Kennedy, D., Kluzek, E., Lawrence, P.J.,
  Li, F., Li, H., Lombardozzi, D., Riley, W.J., Sacks, W.J., Shi, M., Vertenstein, M.,
  Wieder, W.R., Xu, C., Ali, A.A., Badger, A.M., Bisht, G., van den Broeke, M.,
  Brunke, M.A., Burns, S.P., Buzan, J., Clark, M., Craig, A., Dahlin, K., Drewniak, B.,
  Fisher, J.B., Flanner, M., Fox, A.M., Gentine, P., Hoffman, F., Keppel-Aleks, G.,
  Knox, R., Kumar, S., Lenaerts, J., Leung, L.R., Lipscomb, W.H., Lu, Y., Pandey, A.,
  Pelletier, J.D., Perket, J., Randerson, J.T., Ricciuto, D.M., Sanderson, B.M., Slater, A.,
  Subin, Z.M., Tang, J., Thomas, R.Q., Val Martin, M., Zeng, X., 2019. The Community
  Land Model Version 5: Description of New Features, Benchmarking, and Impact of
  Forcing Uncertainty. J. Adv. Model. Earth Syst. 11, 4245–4287. https://doi.org/
  10.1029/2018MS001583.
- Legates, D.R., McCabe, G.J., 1999. Evaluating the use of "goodness-of-fit" measures in hydrologic and hydroclimatic model validation. Water Resour. Res. 35, 233–241. https://doi.org/10.1029/1998WR900018.
- Leite-Filho, A.T., de Sousa Pontes, V.Y., Costa, M.H., 2019. Effects of Deforestation on the Onset of the Rainy Season and the Duration of Dry Spells in Southern Amazonia.
  J. Geophys. Res. Atmos. 124, 5268–5281. https://doi.org/10.1029/2018JD029537.
- Lenton, T.M., Held, H., Kriegler, E., Hall, J.W., Lucht, W., Rahmstorf, S., Schellnhuber, H. J., 2008. Tipping elements in the Earth's climate system. Proc. Natl. Acad. Sci. 105, 1786–1793.
- Levy, M.C., Lopes, A.V., Cohn, A., Larsen, L.G., Thompson, S.E., 2018. Land use change increases streamflow across the arc of deforestation in Brazil. Geophys. Res. Lett. 45, 3520–3530.
- Li, F., Zhang, G., Xu, Y.J., 2014. Spatiotemporal variability of climate and streamflow in the Songhua River Basin. northeast China. J. Hydrol. 514, 53–64.
- Longuevergne, L., Scanlon, B.R., Wilson, C.R., 2010. GRACE hydrological estimates for small basins: Evaluating processing approaches on the High Plains aquifer, USA. Water Resour. Res. 46 https://doi.org/10.1029/2009WR008564.
- Lovejoy, T.E., Nobre, C., 2019. Amazon tipping point: Last chance for action. Sci. Adv. https://doi.org/10.1126/sciady.aba2949.
- Maeda, E.E., Ma, X., Wagner, F.H., Kim, H., Oki, T., Eamus, D., Huete, A., 2017. Evapotranspiration seasonality across the Amazon Basin. Earth Syst. Dyn. 8, 439–454. https://doi.org/10.5194/esd-8-439-2017.
- Malhi, Y., Roberts, J.T., Betts, R.A., Killeen, T.J., Li, W., Nobre, C.A., 2008. Climate change, deforestation, and the fate of the Amazon. Science (80-.) 319, 169–172. https://doi.org/10.1126/science.1146961.
- Mann, H.B., 1945. Nonparametric tests against trend. Econom. J. Econom. Soc. 245–259. Mapbiomas, Amazonia, 2022. Collection 2.0 of annual maps of land cover, land use and land use changes between 1985 to 2018 in the Pan-Amazon, The Amazonian Network of Georeferenced Socio-Environmental Information (RAISG).
- Martens, B., Miralles, D.G., Lievens, H., Van Der Schalie, R., De Jeu, R.A.M., Fernández-Prieto, D., Beck, H.E., Dorigo, W.A., Verhoest, N.E.C., 2017. GLEAM v3: Satellite-based land evaporation and root-zone soil moisture. Geosci. Model Dev. 10, 1903–1925
- Matricardi, E.A.T., Skole, D.L., Costa, O.B., Pedlowski, M.A., Samek, J.H., Miguel, E.P., 2020. Long-term forest degradation surpasses deforestation in the Brazilian Amazon.
- Science (80-.) 369, 1378–1382. https://doi.org/10.1126/SCIENCE.ABB3021.

  Mattos, C.R.C., Hirota, M., Oliveira, R.S., Flores, B.M., Miguez-Macho, G., Pokhrel, Y., Fan, Y., 2023. Double stress of waterlogging and drought drives forest–savanna coexistence. Proc. Natl. Acad. Sci. 120. https://www.pnas.org/doi/abs/10.1073/pnas.2301255120.
- Miguez-Macho, G., Fan, Y., 2012a. The role of groundwater in the Amazon water cycle: 1. Influence on seasonal streamflow, flooding and wetlands. J. Geophys. Res. Atmos. 117, 1–30. https://doi.org/10.1029/2012JD017539.
- Miguez-Macho, G., Fan, Y., 2012b. The role of groundwater in the Amazon water cycle: 2. Influence on seasonal soil moisture and evapotranspiration. J. Geophys. Res. Atmos. 117 https://doi.org/10.1029/2012JD017540.
- Miguez-Macho, G., Fan, Y., Weaver, C.P., Walko, R., Robock, A., 2007. Incorporating water table dynamics in climate modeling: 2. Formulation, validation, and soil moisture simulation. J. Geophys. Res. Atmos. 112 https://doi.org/10.1029/ 2006JD008112.
- Miralles, D.G., Holmes, T.R.H., De Jeu, R.A.M., Gash, J.H., Meesters, A., Dolman, A.J., 2011. Global land-surface evaporation estimated from satellite-based observations. Hydrol. Earth Syst. Sci. 15, 453–469.
- Monteith, J.L., 1965. Evaporation and environment, in: Symposia of the Society for Experimental Biology. Cambridge University Press (CUP) Cambridge, pp. 205–234.
- Moore, N., Arima, E., Walker, R., Ramos da Silva, R., 2007. Uncertainty and the changing hydroclimatology of the Amazon. Geophys. Res. Lett. 34 https://doi.org/10.1029/ 2007GL030157.

- Morrison, E.B., Lindell, C.A., 2011. Active or Passive Forest Restoration? Assessing Restoration Alternatives with Avian Foraging Behavior. Restor. Ecol. 19, 170–177. https://doi.org/10.1111/j.1526-100X.2010.00725.x.
- Morton, D.C., DeFries, R.S., Shimabukuro, Y.E., Anderson, L.O., Arai, E., Del Bon Espirito-Santo, F., Freitas, R., Morisette, J., 2006. Cropland expansion changes deforestation dynamics in the southern Brazilian Amazon. PNAS 103, 14637–14641. https://doi.org/10.1073/pnas.0606377103.
- Nobre, C.A., Borma, L.D.S., 2009. "Tipping points" for the Amazon forest. Curr. Opin. Environ. Sustain. 1, 28–36. https://doi.org/10.1016/j.cosust.2009.07.003.
- Nobre, C.A., Sellers, P.J., Shukla, J., 1991. Amazonian deforestation and regional climate change. J. Clim. 4, 957–988. https://doi.org/10.1175/1520-0442(1991)004<0957:
- Nobre, C.A., Sampaio, G., Borma, L.S., Castilla-Rubio, J.C., Silva, J.S., Cardoso, M., 2016. Land-use and climate change risks in the amazon and the need of a novel sustainable development paradigm. PNAS 113, 10759–10768. https://doi.org/10.1073/ pnas.1605516113.
- Pfeffer, J., Seyler, F., Bonnet, M., Calmant, S., Frappart, F., Papa, F., Paiva, R.C.D., Satgé, F., Silva, J.S.D., 2014. Low-water maps of the groundwater table in the central Amazon by satellite altimetry. Geophys. Res. Lett. 41, 1981–1987. https://agupubs. onlinelibrary.wiley.com/doi/full/10.1002/2013GL059134.
- Pielke, R.A., Cotton, W.R., Walko, R.L., Tremback, C.J., Lyons, W.A., Grasso, L.D., Nicholls, M.E., Moran, M.D., Wesley, D.A., Lee, T.J., Copeland, J.H., 1992. A comprehensive meteorological modeling system-RAMS. Meteorol. Atmos. Phys. 49, 69–91. https://doi.org/10.1007/BF01025401.
- Pokhrel, Y.N., Fan, Y., Miguez-Macho, G., Yeh, P.J.F., Han, S.C., 2013. The role of groundwater in the Amazon water cycle: 3. Influence on terrestrial water storage computations and comparison with GRACE. J. Geophys. Res. Atmos. 118, 3233–3244. https://doi.org/10.1002/jgrd.50335.
- Pokhrel, Y.N., Fan, Y., Miguez-Macho, G., 2014. Potential hydrologic changes in the Amazon by the end of the 21st century and the groundwater buffer. Environ. Res. Lett. 9, 84004. https://doi.org/10.1088/1748-9326/9/8/084004.
- Poorter, L., Craven, D., Jakovac, C.C., van der Sande, M.T., Amissah, L., Bongers, F., Chazdon, R.L., Farrior, C.E., Kambach, S., Meave, J.A., 2021. Multidimensional tropical forest recovery. Science (80-.) 374, 1370–1376.
- Priestley, C.H.B., Taylor, R.J., 1972. On the assessment of surface heat flux and evaporation using large-scale parameters. Mon. Weather Rev. 100, 81–92.
- Running, S., Mu, Q., Zhao, M., Moreno, A., 2021. MODIS/Terra Net Evapotranspiration 8-Day L4 Global 500m SIN Grid V061, NASA EOSDIS Land Processes DAAC.
- Salati, E., Dall'Olio, A., Matsui, E., Gat, J.R., 1979. Recycling of water in the Amazon basin: an isotopic study. Water Resour. Res. 15, 1250–1258. https://agupubs.online library.wiley.com/doi/abs/10.1029/wr015i005p01250.
- Sampaio, G., Nobre, C., Costa, M.H., Satyamurty, P., Soares-Filho, B.S., Cardoso, M., 2007. Regional climate change over eastern Amazonia caused by pasture and soybean cropland expansion. Geophys. Res. Lett. 34 https://doi.org/10.1029/ 2007GL030612.
- Schellnhuber, H.J., 2009. Tipping elements in the Earth System. PNAS 106, 20561–20563. https://doi.org/10.1073/pnas.0911106106.
- Sen, P.K., 1968. Estimates of the regression coefficient based on Kendall's tau. J. Am. Stat. Assoc. 63, 1379–1389. https://www.tandfonline.com/doi/abs/10.1080/01621 459,1968.10480934.
- Shukla, J., Nobre, C., Sellers, P., 1990. Amazon deforestation and climate change. Science (80) 247, 1322–1325. https://doi.org/10.1126/science.247.4948.1322.
- Siqueira, V.A., Paiva, R.C.D., Fleischmann, A.S., Fan, F.M., Ruhoff, A.L., Pontes, P.R.M., Paris, A., Calmant, S., Collischonn, W., 2018. Toward continental hydrologichydrodynamic modeling in South America. Hydrol. Earth Syst. Sci. 22, 4815–4842. https://doi.org/10.5194/hess-22-4815-2018.

- Soares-Filho, B.S., Nepstad, D.C., Curran, L.M., Cerqueira, G.C., Garcia, R.A., Ramos, C. A., Voll, E., McDonald, A., Lefebvre, P., Schlesinger, P., 2006. Modelling conservation in the Amazon basin. Nature 440, 520–523. https://doi.org/10.1038/nature04389
- Spracklen, D.V., Arnold, S.R., Taylor, C.M., 2012. Observations of increased tropical rainfall preceded by air passage over forests. Nature 489, 282–285. https://doi.org/ 10.1038/nature11390.
- Staal, A., Tuinenburg, O.A., Bosmans, J.H.C., Holmgren, M., Van Nes, E.H., Scheffer, M., Zemp, D.C., Dekker, S.C., 2018. Forest-rainfall cascades buffer against drought across the Amazon. Nat. Clim. Chang. 8, 539–543. https://doi.org/10.1038/s41558-018-0177-y.
- Staal, A., Fetzer, I., Wang-Erlandsson, L., Bosmans, J.H.C., Dekker, S.C., van Nes, E.H., Rockström, J., Tuinenburg, O.A., 2020. Hysteresis of tropical forests in the 21st century. Nat. Commun. 11, 1–8. https://doi.org/10.1038/s41467-020-18728-7.
- Staver, A.C., Archibald, S., Levin, S.A., 2011. The global extent and determinants of savanna and forest as alternative biome states. Science (80-.) 334, 230–232. https:// doi.org/10.1126/science.1210465.
- Theil, H., 1950. A rank-invariant method of linear and polynomial regression analysis. Indag, Math. 12, 173.
- Van Der Ent, R.J., Savenije, H.H.G., Schaefli, B., Steele-Dunne, S.C., 2010. Origin and fate of atmospheric moisture over continents. Water Resour. Res. 46 https://doi.org/ 10.1029/2010WR009127.
- van Nes, E.H., Arani, B.M.S., Staal, A., van der Bolt, B., Flores, B.M., Bathiany, S., Scheffer, M., 2016. What do you mean, 'tipping point'? Trends Ecol. Evol. 31,
- Walker, R.T., 2020. Collision course: development pushes amazonia toward its tipping point. Environ. 63, 15–25. https://doi.org/10.1080/00139157.2021.1842711.
- Walko, R.L., Band, L.E., Baron, J., Kittel, T.G.F., Lammers, R., Lee, T.J., Ojima, D., Pielke, R.A., Taylor, C., Tague, C., Tremback, C.J., Vidale, P.L., 2000. Coupled atmosphere-biophysics-hydrology models for environmental modeling. J. Appl. Meteorol. 39, 931–944. https://doi.org/10.1175/1520-0450(2000)039<0931: CABHMF>2.0.CO;2.
- Weng, W., Luedeke, M., Zemp, D., Lakes, T., Kropp, J., 2018. Aerial and surface rivers: Downwind impacts on water availability from land use changes in Amazonia. Hydrol. Earth Syst. Sci. 22, 911–927. https://doi.org/10.5194/hess-22-911-2018.
- Werth, D., Avissar, R., 2005. The local and global effects of Southeast Asian deforestation, Geophys. Res. Lett. 32, 1–4, https://doi.org/10.1029/2005GL022970.
- Xu, D., Agee, E., Wang, J., Ivanov, V.Y., 2019. Estimation of evapotranspiration of Amazon rainforest using the maximum entropy production method. Geophys. Res. Lett. 46, 1402–1412.
- Yamazaki, D., Kanae, S., Kim, H., Oki, T., 2011. A physically based description of floodplain inundation dynamics in a global river routing model. Water Resour. Res. 47 https://doi.org/10.1029/2010WR009726.
- Zak, R., Nippert, J.B., 2012. Comment on "Global resilience of tropical forest and Savanna to critical transitions". Science (80-.) 336, 232–235. https://doi.org/ 10.1126/science.1219346.
- Zemp, D.C., Schleussner, C.F., Barbosa, H.M.J., Hirota, M., Montade, V., Sampaio, G., Staal, A., Wang-Erlandsson, L., Rammig, A., 2017. Self-amplified Amazon forest loss due to vegetation-atmosphere feedbacks. Nat. Commun. 8, 1–10. https://doi.org/10.1038/ncomms14681.
- Zeng, N., 1999. Seasonal cycle and interannual variability in the Amazon hydrologic cycle. J. Geophys. Res. Atmos. 104, 9097–9106. https://doi.org/10.1029/ 1998 ID200088
- Zeng, N., Dickinson, R.E., Zeng, X., 1996. Climatic impact of Amazon deforestation A mechanistic model study. J. Clim. 9, 859–883. https://doi.org/10.1175/1520-0442 (1996)009<0859:CIOADM>2.0.CO:2.